Mechanical Systems and Signal Processing 238 (2025) 113128

Contents lists available at ScienceDirect

Mechanical Systems and Signal Processing

journal homepage: www.elsevier.com/locate/ymssp

Full length article

Predictive control algorithm for the Adaptive Tuned Particle Impact Damper

Mateusz Żurawski [a,*], Cezary Graczykowski [b], Robert Zalewski [a]

[a] Institute of Machine Design Fundamentals, Warsaw University of Technology, Warsaw, Poland
[b] Institute of Fundamental Technological Research, Polish Academy of Sciences, Warsaw, Poland

ARTICLE INFO

Communicated by J.C. Ji

Keywords:
Mechanical vibrations
Adaptive damping
Adaptive Tuned Particle Impact Damper
Experimental and numerical investigations
Contact forces
Predictive control algorithm

ABSTRACT

This paper presents a novel predictive control strategy for the Adaptive Tuned Particle Impact Damper (ATPID), aimed at improving vibration suppression in systems with limited available information. The proposed control algorithm, called the Predictive Control Algorithm (PCA), is based on the prediction and optimization of system dynamics and operates effectively even when system parameters and external excitations are unknown. The only available input for the control process is the measured vibration response of the system. Under this constraint, the PCA accurately estimates the optimal height of the damper in real time, achieving vibration reduction of up to 75%. The algorithm also exhibits a second operational mode: when a theoretical model of the mechanical system is available, the PCA can incorporate this additional knowledge to further enhance control accuracy and performance. The algorithm's two operating approaches enable its application in a wide range of engineering environments. The robustness of the approach is further validated through sensitivity analyses investigating the impact of variations in particle mass, excitation amplitude, and gravitational conditions. The results obtained from the PCA algorithm show that the height prediction error remains below 10%, with accuracy increasing in conditions of higher excitation and particle mass. The main novelty of this work is the development of a versatile and fully adaptive predictive control algorithm for ATPID systems, capable of optimizing damper parameters based solely on vibration feedback but also leveraging mathematical system models when available. The proposed control algorithm represents important progress in the development of adaptive mechanical structures employing particle impact damping technology.

1. Introduction

Mechanical vibrations are a common phenomenon in various mechanical systems, ranging from simple spring arrangements to complex engineering structures. In most cases, they result from transformation of kinetic and potential energy between individual elements of the system. Even the slightest vibrations can lead to material wear, performance degradation, and in extreme situations, a system failure. Therefore, understanding the nature, and effects of mechanical vibrations is crucial for engineers striving to design systems that are optimal in terms of performance, durability and safety. Mechanical systems are becoming increasingly complex and the requirements imposed on them are growing. The development of methods for damping mechanical vibrations is an ongoing field of the scientific and engineering research. Traditional damping methods, such as viscous dampers or vibration isolators, are still widely employed and effective in many applications. However, with technological advancements, a need for more advanced and

* Corresponding author.
E-mail address: Mateusz.Zurawski@pw.edu.pl (M. Żurawski).

https://doi.org/10.1016/j.ymssp.2025.113128
Received 11 February 2025; Received in revised form 13 May 2025; Accepted 16 July 2025
Available online 1 August 2025

adaptive damping techniques that can adjust to changing operating conditions and environments has arisen. These new approaches, based on the principles of adaptive control, that enable more effective and flexible damping of mechanical vibrations, are an attractive area for research and engineering applications.

Particle dampers (PD) are a practical solution for reducing vibrations in technical applications across different fields. They are constructed by filling containers attached to the vibrating structure by particles or placing them within the structure's voids. During structural vibrations, the momentum of vibrating structure is transferred to the particles, initiating interaction within the granular material [1–3]. Friction and inelastic collisions between the particles result in energy dissipation within the damper and an effective decrease of structural vibrations [4–8]. In [9], the influence of container design on particle damper effectiveness was examined across various levels of random excitation. Experimental investigation utilized a single-story structure featuring a low fundamental frequency. Different container configurations, including single and dual compartments, were analyzed to assess their impact on the damper performance. Previous research has indicated that the damping efficiency of a particle damper relies on various factors, including particle size, shape, type of granular material and filling ratio [10–12]. Among these parameters, the choice of granular material significantly affects the reduction of vibration amplitudes in mechanical structures [13]. This study seeks to examine the impact of 20 various granular materials on vibration attenuation. The materials were categorized into two main groups: soft particles such as rubber granulate and hard particles like steel balls. Moreover, the paper proposes a hybrid particle damper, incorporating mixtures of two different granular materials, such as combining soft and hard particles. Additionally, mathematical and numerical modeling plays a crucial role in understanding the dynamic behavior of particle systems, aiding the design and optimization of damping mechanisms in order to the enhance equipment performance and prolong its lifespan [14–18]. By utilizing the physical principles of the Kelvin–Voigt model, paper [19] introduces a continuous contact formulation that incorporates varying viscous damping coefficients. A lot of theoretical models for the particle damper relies on observations of vibration phenomena, but does not directly unveil the damping mechanism.

Paper [20] presents the multiple unidirectional single-particle damper (MUSPD), establishing its mechanical model and proposing a corresponding numerical simulation method whose validation is achieved through a shaking table test. Furthermore, an equivalent mechanical model for the MUSPD, based on an analysis of its damping mechanism, provides analytical solutions. A method for optimizing the MUSPD's performance under dynamic loads is then proposed. Numerical simulations confirm the accuracy of the model and the effectiveness of the optimization method, highlighting the MUSPD's fine damping effect and the feasibility of proposed approaches. The subject of Impact Damper optimization can also be found in papers [21,22]

Particle dampers are comprehensive tools in mechanical engineering, exhibiting a broad range of applications in mitigating undesired vibrations across various systems. The paper [23] presents a coupled multi-body dynamics — discrete element method designed to simulate the damping characteristics of a damper–cable system subjected to harmonic excitation. Study presented in paper [24] explores the application of a particle damper featuring energy harvesting capabilities for vibration control of structures, and further examines the correlation between control and energy capture. Key parameters influencing vibration control and energy harvesting, including harmonic excitation frequency, motion distance, particle filling ratio and particle size, are investigated through a single-degree-of-freedom model experiment. The results indicate that the maximum vibration attenuation rate is achieved when the filling ratio of particles is 60%. Furthermore, as motion distance increases, the effectiveness of vibration control tends to decrease, while the energy harvesting capability tends to increase.

In contemporary additive manufacturing processes such as laser powder bed fusion (LPBF), residual unmelted powder intentionally remains within structures, effectively producing integrated (with the based system) particle dampers. While the efficacy of particle damping has been convincingly demonstrated in the current research, the applicability of the findings in such structures remains somewhat limited. The paper [25] experimentally investigates the effects of particle damping on beam structures fabricated using LPBF with AlSi10Mg alloy. Performance curves for various beam parameter sets are evaluated to assist designers in estimating damping effects using the provided data. Damping characteristics are determined through experimental modal analysis using impulse excitation, with response assessment conducted in the frequency domain, focusing primarily on the first bending mode of vibration. Moreover, significantly enhanced damping, up to 20 times greater, is observed in particle-filled cavities compared to identical components without such damping measures. Additional studies of the particle damping implemented in structures produced using additive manufacturing techniques can be found in [26–28].

The risk for blast impact loads affecting bridge structures is progressively rising. However, the precise laws governing the local and overall explosion response of concrete box girder bridges remain elusive, and there is a shortage of anti-explosion devices aimed at reducing the overall explosion response of bridges. Investigation presented in paper [29] describes a rotational inertial particle damper (R-IPD) which was designed and integrated into a 1:4 scale model of a typical three-span continuous girder bridge. Papers [30,31] present a particle tuned mass damper (PTMD) attached to a Multi Degree of Freedom structure of high-rise building, subjected to wind excitation. The model was developed using an equivalent simplified method, and simulation results were validated through wind tunnel experiments. The analysis encompasses the changes of energy within the entire structural system, and energy dissipation resulting from structural damping and external input energy. In general, the operating principle of such a device is analogous to the behavior of Adaptive-Passive Tuned Mass Damper [32]. Such device can be used to reduce vibrations in buildings [33–36]. Studies of analogical systems subjected to seismic excitation and wind-induced vibration were presented in [37,38]. The newest and actual researches focus on modeling PID dampers and their damping characteristics using artificial intelligence algorithms. In [39], the potential of replacing the model based on the Leidenfrost phenomenon describing the operation principle of a damper working under specific conditions was presented. It turns out that it is possible to use an algorithm based on artificial neural networks to effectively represent the behavior of the PID damper. Another study that enables the modeling of granular behavior in a specific working environment using the Leidenfrost model is presented in the paper [40].

In [41], the proposed particle damper exhibits hysteresis under dynamic excitation, with the hysteresis loops varying according to the excitation frequency due to its nonlinear behavior. A neural network was introduced to model this phenomenon, effectively capturing the nonlinear relationships involved. Similarly, studies such as [42–44] investigated vibrations in printed circuit boards, proposing neural networks to describe and predict the efficiency of vibration reduction using particle dampers, relying exclusively on experimental studies. Existing research indicates that artificial neural networks are predominantly utilized to determine parameters for vibration reduction in particle dampers. However, these approaches are generally based either on experimental data alone or on theoretical models limited to specific motion scenarios, often characterized by the Leidenfrost effect.

Research on PID dampers has been conducted for decades. A novel experimental data techniques are being utilized and the latest modeling methods are employed. However, it turns out that in many cases proposed designs do not appear to be more efficient than common technical solutions enabling vibration damping. This is because in the proposed designs, all parameters influencing the damping efficiency remain constant during the absorber's operation. On the other hand, in most cases, the excitations to which mechanical systems are subjected vary over time. This aspect causes that devices aimed at effectively reducing generated vibrations should adapt to the current operating conditions. At this context, it is worth mentioning a series of studies by the research team under the supervisor of Prof. Masri [45–51]. In these studies, the research on the principle of operation of the PID damper was presented, and situations in which the most effective vibration damping occurs were identified. However, it should be noted that the proposed research setup generally allowed for the analysis of horizontal motion, resulting in the elimination of the influence of gravity during the modeling stage. This simplification leads to a lack of description of the behavior of the granulate when it moves vertically, where gravity plays a crucial role. Additionally, in the proposed damper construction, limiting the movement of the moving mass in one direction was achieved by immediately extending the stoppers. Such a solution allowed for blocking but not accelerating the moving mass.

The response to all these problems was a technical solution presented by the authors in the paper [52] where a device called the Adaptive Tuned Particle Impact Damper (ATPID) was proposed. This damper consists of a container, a single grain, and a movable upper wall (ceiling) which movement is controlled by an electric engine connected to a control system. The rotational motion of the engine shaft was converted into reciprocating motion of the upper wall. As a result, the volume of the damper in where the grain moved could be changed in real time, which is crucial for changing the damper's characteristics. Experimental studies, modeling of the damper using the theory of soft contact, sensitivity analysis of the system and parametric optimization were presented. All these studies allowed for the presentation of a simple control algorithm based on iterative search of the solution space, which enables finding the optimal damper height from a damping point of view. Unfortunately, it has many drawbacks, including a relatively long search time. At this stage, the authors decided that it is necessary to propose a new, more efficient control method for the ATPID damper so it can become a fully adaptive device.

A potential solution to the challenges outlined above is application of Model Predictive Control (MPC) [53,54]. In this approach, a mathematical model of the system under consideration is used to repeatedly solve an optimization problem formulated at consecutive time intervals of predefined durations. The high effectiveness of the MPC method results from sequential update of control, which enables compensation of inaccuracies in mathematical model as well as accounting for changes in external excitations and process disturbances. The MPC approach is successfully applied across various systems in numerous branches of engineering. The exemplary applications include the control of semi-active car suspension where unknown road roughness is estimated by the controller [55], the control of suspension with electro-rheological dampers providing trade-off between comfort and handling performance [56] and the development of optimal switching sequence for multi-mode dampers in air suspension equipped with solenoid valves [57]. Moreover, MPC is extensively utilized in the control of motion of diverse actuators and manipulators. The examples include the robust optimal control of robot arm under actuator fault conditions [58] or the control of system of hybrid actuators applied in artificial muscles [59]. In the case of impact mitigation problems, MPC combined with genetic algorithm serving as optimization solver was applied to control semi-active landing gear [60]. Additionally, the class of state-dependent path-tracking methods integrates MPC with various identification procedures and other control techniques. These methods include application of predictive models with equivalent time-varying quantities to replace simultaneously occurring unknown parameters and excitations [61] as well as methods for sequential disturbance identification, prediction and compensation [62]. On the other hand, application of MPC for vibrating systems equipped with impact dampers has neither been investigated nor implemented so far.

Based on the conducted literature review, a substantial research gap can be identified in the field of Particle Impact Dampers (PIDs) for vibration suppression. While numerous experimental and numerical studies have investigated the influence of various damper parameters on vibration mitigation effectiveness, the majority of the proposed solutions remain limited in terms of adaptability and real-time responsiveness. Prior research has demonstrated the broad applicability of PIDs in structures subjected to impacts, seismic events, and harmonic excitations near resonance [63]. These studies have highlighted that key factors affecting damping efficiency include the mass of the free-moving particles, the container volume, and the various types of excitations. In addition, researchers have explored structural enhancements, such as the integration of energy harvesting mechanisms, and have formulated optimization strategies aimed at improving vibration suppression [64]. However, most of these designs are inherently passive and lack the ability to adjust damper parameters dynamically during their operation. The most pronounced research gap is the absence of PID systems capable of semi-active or adaptive control, particularly in scenarios involving unexpected or unpredictable changes in excitation. To date, no efficient algorithms have been proposed that can rapidly determine the optimal container volume in response to time-varying external excitations such as sudden wind gusts, seismic shocks, mechanical impacts, or other unforeseen excitations commonly encountered in real-world environments.

This article extends the research presented in paper [52] by proposing the Predictive Control Algorithm (PCA), which can be effectively applied to control the operation of the ATPID damper. The main contribution of the paper is the development of the

control algorithm which allows to predict response of the system and quickly determine the optimal device height without the knowledge of any system or excitation parameters. As a result, it can be applied when excitation or system properties are rapidly changing in time, providing full adaptivity of the ATPID damper. Initially, the general idea of the PCA algorithm is described, and the applied procedure for calculating the optimal damper height is explained in details. Then, the application of the algorithm in a damper connected to unknown mechanical system in terms of number of degrees of freedom, stiffness, mass, damping, etc. is presented. Further, the operation of the algorithm is described in detail in the situation where properties of the mechanical system are known and there is a possibility of its exact mathematical modeling. Finally, a sensitivity analysis of the algorithm is performed, and its effectiveness is determined.

2. Predictive control algorithm for the ATPID damper

The Adaptive Tuned Particle Impact Damper builds upon the classical Particle Impact Damper concept, which consists of a container filled with grains [65] (see Fig. 1). The ATPID damper features a cylindrical chamber containing a single Polylactide grain. A movable plate, connected via screw joints and a clutch, is driven by a compact electric motor. The motor is powered by a voltage range of 3 V to 6 V. Under no load, it consumes 30 mA at 3 V and measures 15 × 30 mm. The rotational motion of the shaft is converted into a vertical linear displacement of the plate (ceiling). This enables real-time adjustment of the internal volume of the damper by shifting the upper wall relative to the fixed lower wall (floor). A simple electromechanical system controls the motor's operation, including direction and speed of motion. This allows dynamic tuning of the particle's working space, directly affecting damping performance. A detailed description of the ATPID prototype is presented in the previously published paper [52].

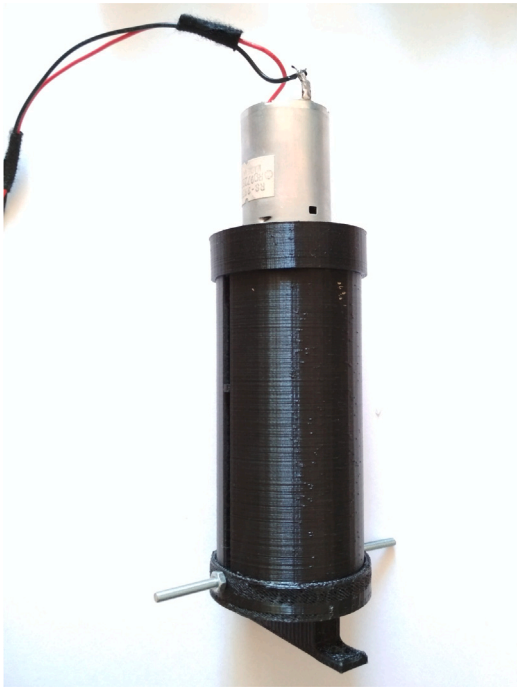

Fig. 1. Prototype of the adaptive tuned particle impact damper.

The ATPID includes a cylindrical container with a single particle made of Polylactide (PLA) enclosed inside the damper. The adjustable ceiling is connected to an electric motor via screw mechanisms and a clutch system. The motor's rotational movement is converted into vertical motion, enabling precise control of the ceiling's position, movement direction, and velocity. This electromechanical system provides a simple and effective solution for dynamically tuning the damper's geometry, allowing for real-time adaptation to changing conditions and enhancing vibration damping efficiency. When subjected to external excitation, the grain inside moves and collides with the container walls. These collisions dissipate energy, reducing the vibration amplitudes of the mechanical system to which the damper is attached. A key parameter influencing the damping performance of the particle damper is the container height. To enhance functionality, the ATPID introduces a design that allows real-time control of the container ceiling's position. This enables dynamic adjustment of the distance between the lower and upper walls of the damper, effectively tuning the timing and velocities of collisions, influencing the energy dissipation process, and optimizing the system's performance. The main challenge related to the ATPID damper is to propose an effective algorithm that allows computing the optimal damper height. This problem is thoroughly resolved in the following sections of this paper.

Analysis of the dynamics of various mechanical systems is a crucial aspect of research which allow to determine the principles of their operation. Each mechanical system is characterized by material, geometric and other physical properties that influence

its dynamic characteristics. When all the system parameters are known, it becomes possible to analyze the dynamic response of vibrations applying two different methods. The first is the experimental investigations which enable determining the oscillations of the structure using a professional measurement setup. In the second approach, the dynamic response of the construction can be studied through an appropriate numerical modeling of such a system and by performing computer simulations. A schematic description of this classical method for analyzing the dynamic response of any mechanical system is presented in Fig. 2.

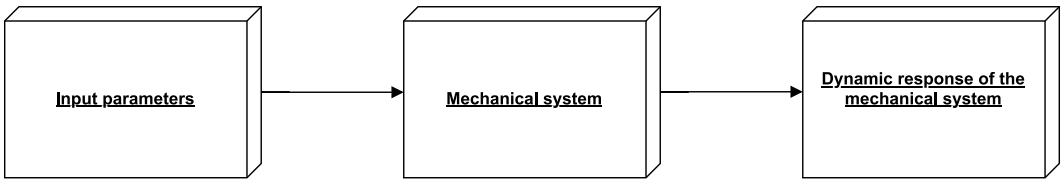

Fig. 2. Scheme of the classical approach of the analysis of the mechanical system dynamic response.

Let us consider a cantilever beam with an ATPID damper connected to its free end (Fig. 8) as the mechanical system under discussion. The entire structure is subjected to the kinematic excitation and resonant-harmonic vibrations. This implies that the input parameters describing the considered system are as follows: the amplitude and the frequency of excitation, the length, width and height of the beam, the density and other material properties, the diameter and material properties of the applied ATPID grain and the height of the ATPID damper.

By using experimental or numerical investigations, the displacement of the beam free end vibrations can be determined. One of the important problems is determining the optimal height of the ATPID damper providing the most effective damping under the currently occurring excitation. Obtaining such information requires performing a large number of measurements or simulations for different values of the damper height within a wide range of data. As a result, it becomes possible to identify the damper height value that causes the most effective reduction of the amplitude of the system's vibrations. However, such an approach, especially in experimental studies, is often time-consuming and inefficient for rapid vibration mitigation.

In light of this, a novel Predictive Control Algorithm (PCA) has been proposed, to enable fast and efficient determination of the optimal damper height that allows for the most effective mitigation of system vibrations. The general idea of the PCA algorithm is illustrated in Fig. 3 and described comprehensively in the subsequent sections of the manuscript.

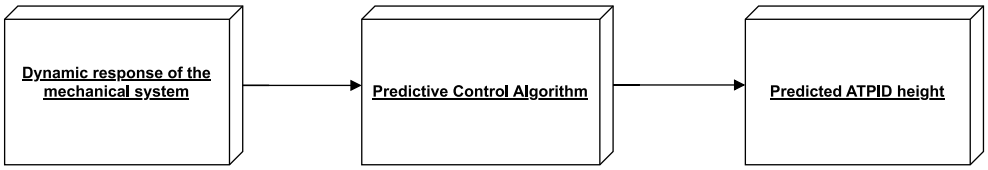

Fig. 3. Scheme of the general idea of the PCA algorithm.

The concept behind the Predictive Control Algorithm aims to address the inverse problem to the classical analysis of the dynamics of a mechanical system as presented in Fig. 2. By utilizing an input data in the form of the desired system response of the cantilever beam and employing the innovative PCA block, the appropriate height of the ATPID damper for which the system's response will resemble the one provided to the algorithm can be determined. The Predictive Control Algorithm encompasses several assumptions corresponding to the criteria that describe the characteristic movement of the granular material, at which optimal system damping occurs. In the ideal approach, it is necessary to input the system's vibration response that would occur at the optimal damper height into the PCA block. Consequently, the control algorithm will allow to determine the aforementioned optimal damper height. However, in practice, predicting oscillations in this characteristic state proves challenging, and often unattainable, leading to difficulties in obtaining precise predictions. Consequently, the analysis will be based on the system vibration responses that differ from the optimal ones. The magnitude of the observed deviation in the input data will directly influence the error in the obtained damper's height. Repetitive application of the PCA algorithm will result in an increased efficiency of the proposed method.

2.1. Assumptions and initiation of the predictive control algorithm

The Predictive Control Algorithm consists of input data (dynamic response of the mechanical system) and assumptions based on criteria describing the optimal movement of ATPID grain for which the system's oscillations experience the greatest damping. These assumptions have been preliminary formulated in the manuscript [52], derived from a comprehensive sensitivity analysis of the system. An exemplary plot illustrating the optimal grain movement is presented in Fig. 4. Necessary conditions for the optimal grain movement are as follows:

- impacts occur when the direction of the primary system movement is opposite to the direction of the grain movement,
- impacts occur when the velocity of the primary system is maximal or when its velocity decreases,

- impacts occur in every period of vibrations since otherwise, the system response will be unstable,
- the sticking effect between grain and walls should be avoided.

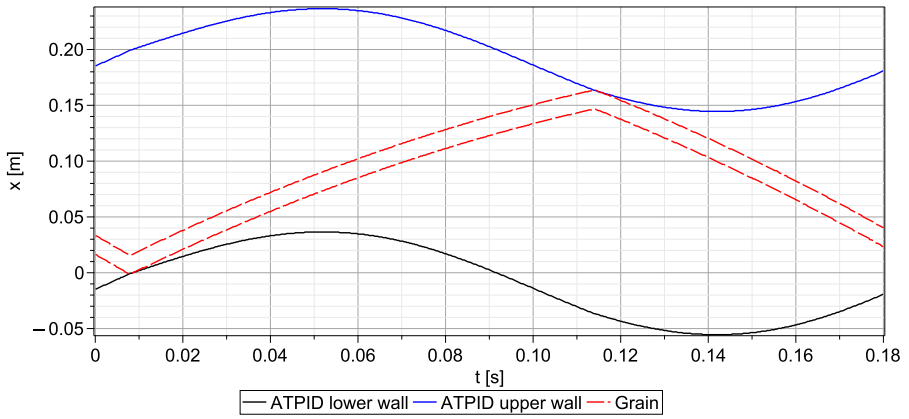

Fig. 4. A representative example of optimal grain movement inside the damper during one period of vibration.

The conditions for optimal grain movement delineate a wide set of the results in which the best solution has to be identified. Depending on the specific scenario being examined, the optimal value of damper's height may align more closely with one of the above stated necessary condition or the other. To preliminarily refine the solution set within the PCA framework, a simplification of the optimal movement conditions for the granulate was implemented. This analysis focuses on scenarios where collisions are required to occur when the primary system's velocity reaches its maximum. Following this, further adjustments are made to determine the final optimal height of the damper. The latter process facilitates the extension of the analysis to include situations where the primary structure's velocity is either at its maximum or is decreasing. Taking the above into account, a Predictive Control Algorithm procedure can be constructed as follows:

Minimize: $max(x_s^d)$

with respect to: h_{max}

subject to: system governing equations

$$\xi_{c_1}(t_{c_1}) > 0 \quad <=> \quad \dot{x}_s \quad > 0 \quad and \quad \dot{x}_g < 0 \tag{1}$$

$$\xi_{c_2}(t_{c_2}) > 0 \quad <=> \quad \dot{x}_s \quad < 0 \quad and \quad \dot{x}_g > 0 \tag{2}$$

$$\xi_{c_1}(t_{c_1}) > 0 \quad or \quad \xi_{c_2}(t_{c_2}) > 0 \quad <=> \quad |\dot{x}_s| \quad is \quad maximal \tag{3}$$

$$\xi_{c_1}(t_{c_1}) > 0 \quad or \quad \xi_{c_2}(t_{c_2}) > 0 \quad \quad in \quad every \quad period \quad of \quad vibrations \tag{4}$$

$$t_c < \frac{\gamma}{2} T \tag{5}$$

where $max(x_s^d)$ - maximal champlitude of system vibration in the damped state, h_{max} - ATPID damper height, ξ_{c_1} and ξ_{c_2} - overlaps (contact indicators) between grain and walls, $\dot{x}_s$ and $\dot{x}_g$ - system and grain velocities, γ - the coefficient defining time of contact t_c, $\gamma \ll 1$ and for this case it is assumed as $\gamma \approx 0.1$, T - one period of beam oscillation, t_{c_1} and t_{c_2} - times of impact of the particle with the lower and upper walls. System governing equations can be used only in the situation when all the parameters of the experimental test stand are known and it can be described by theoretical model.

The Predictive Control Algorithm analyzes the movement of the grain in the ATPID container and determines the optimal height of the damper. To achieve the final forms of solutions, the model for PCA calculations (Fig. 5) and its detailed mathematical description are presented, considering the earlier introduced assumptions (Eqs. (6)–(15)).

The general assumption is that the floor of the ATPID damper is attached to a structure subjected to harmonic vibrations. As a result of these vibrations, the lower part of the enclosure oscillates in a manner analogous to the entire structure at the attachment point. Hence, the displacement of this damper component can be described in a general form by the following equation:

$$x_{pred}^s = A_{pred} sin(2\pi f t) \tag{6}$$

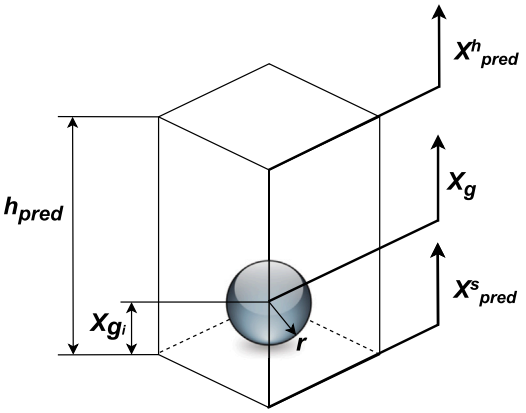

Fig. 5. Scheme of the model for Predictive Control Algorithm calculations.

where A_{pred} - predicted (or measured) amplitude of the system vibration response, f - excitation frequency. According to Eq. (6), the displacement of the ceiling of the ATPID damper container can be calculated as:

$$x^h_{pred} = x^s_{pred} + h_{pred} \tag{7}$$

where h_{pred} is the predicted ATPID damper height. At this stage, h_{pred} is treated as the unknown parameter, and the primary objective of the algorithm is to find this value. In the subsequent step of the procedure, it becomes necessary to set the initial conditions for the calculation and identify the location of the beam where contact with the grain takes place. This involves determining the times of impact of the particle with the lower and upper walls of the container, denoted as t_{c_1} and t_{c_2}, respectively. The displacement of the beam during the times t_{c_1} and t_{c_2} can be described using the following equations:

$$x^s_{pred}(t_{c_1}) = A_{pred} sin(2\pi f t_{c_1}) \tag{8}$$

$$x^h_{pred}(t_{c_2}) = A_{pred} sin(2\pi f t_{c_2}) + h_{pred} \tag{9}$$

The initial position of the particle is defined by the position of the lower container wall at the moment of impact:

$$x_{g_i} = x^s_{pred}(t_{c_1}) + r = A_{pred} sin(2\pi f t_{c_1}) + r \tag{10}$$

Following the impact, the grain is anticipated to move without any subsequent collisions, and its motion can be represented as uniformly decelerated. Consequently, the equation describing the grain displacement at time t_{c_2} will have the following form:

$$X_g = x_{g_i} + V_{k_0}(t_{c2} - t_{c1}) - \frac{g(t_{c_2} - t_{c_1})^2}{2} \tag{11}$$

where V_{k_0} is the initial velocity of the grain and g is the gravity. The collision of the grain with the upper wall of the damper will occur when:

$$X_g + r = x^h_{pred}(t_{c_2}) \tag{12}$$

Substituting Eqs. (9) and (11) into Eq. (12), the general form is as follows:

$$r + A_{pred} sin(2\pi f t_{c1}) + V_{k_0}(t_{c2} - t_{c1}) - \frac{g(t_{c2} - t_{c1})^2}{2} + r = A_{pred} sin(2\pi t_{c2}) + h_{pred} \tag{13}$$

By transforming the Eq. (13), the predicted height of the ATPID damper takes the form:

$$h_{pred} = 2r + A_{pred} sin(2\pi f t_{c1}) + V_{k_0}(t_{c2} - t_{c1}) - \frac{g(t_{c2} - t_{c1})^2}{2} - A_{pred} sin(2\pi f t_{c2}) \tag{14}$$

Based on the previously introduced algorithm assumptions, the collision with the bottom part of the container, without sticking effect, happens when the beam's velocity is at its maximum: $2\pi f t_{c_1} = 0$. As a result, the first impact time occurs when $t_{c_1} = 0$ and then $x^s_{pred}(t_{c_1}) = 0$. Assumption of the time t_{c_2} at which the grain will collide with the upper part of the container results from introduction of optimality criteria which indicates that, in the case of optimal particle movement, two collisions with ceiling and the floor take place during one vibration period. Thus, the second collision must occur when: $2\pi f t_{c_2} = \pi$ and consequently $t_{c_2} = \frac{1}{2f}$. Taking into account such an assumptions, the Eq. (14) has a simplified form:

$$h_{pred} = 2r + V_{k_0}\left(\frac{1}{2f}\right) - \frac{g\left(\frac{1}{2f}\right)^2}{2} \tag{15}$$

In this manuscript, two different cases of implementing the Predictive Control Algorithm for the ATPID damper are considered. In the first scenario, it is assumed that there is a lack of detailed information about the mechanical system to which the damper is connected. This means that the only information that can be obtained is the kinematic excitation displacement and the beam's vibration response at the damper attachment point, using the laser sensor. Additionally, in this approach, it is not possible to propose any numerical model of the test stand. The second case discussed in the manuscript is a situation where all parameters describing the basic vibrating structure are known. This allows to propose a model that can predict the beam's vibration response in a characteristic state. Detailed descriptions of both methods are presented in subsequent parts of the manuscript. However, it is essential to note that both considered in the manuscript cases involve calculations based solely on the measured excitation amplitude and dynamic behavior of the vibrating beam at the damper attachment point (kinematics of the grain is not measured). On the other hand, based on Eqs. (14) and (15), it can be noticed that the calculations require the velocity V_{k_0} acquired by the grain after collision with the lower part of the damper. This means that a special method to estimate the grain's velocity based on the beam's displacements or velocities must be proposed. For this purpose, a numerical model used in the paper [52] which assumes soft contact between the container and the grain was effectively applied. Inthe proposed method, the vibrating beam is connected with the ATPID damper with preliminarily determined optimal container height. Computer simulations allow to analyze how the velocity of both the beam and the grain changes, especially when both elements collide. A series of calculations for different variants of the described problem was performed. The result of a selected case is presented in Fig. 6.

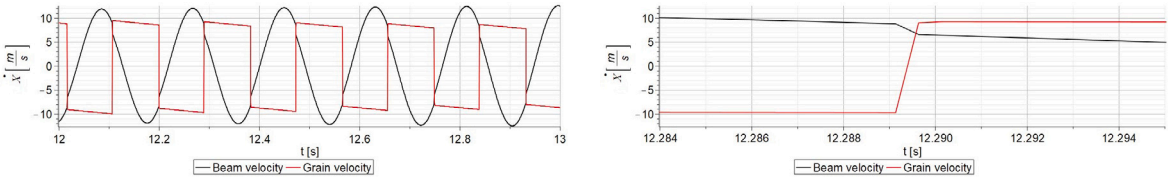

(a) General changes of the velocities (b) Detailed changes of the velocities

Fig. 6. Change of the grain and beam velocity during the vibration.

Upon detailed examination of Figs. 6(a) and 6(b), it becomes evident that when the grain impacts the container floor or ceiling, it attains a velocity similar to that of the beam before the collision. Building on these observations, it is hypothesized that the particle's initial velocity will be considered equal to the beam's velocity at the moment of collision, denoted as t_{c_1}. This assumption can be expressed by the following formula:

$$V_{k_0} = \dot{x}^s_{pred}(t_{c_1}) = 2\pi f A_{pred} \tag{16}$$

Determined initial velocity of the particle allows to compute predicted height of the damper according to Eq. (15).

2.2. PCA implementation for the unknown mechanical system

In this case the only available information about the considered system is how it vibrates at the damper's attachment point. The schematic representation of this case is presented in Fig. 7.

In this approach, the analysis is based solely on experimental investigations. The mechanical system, represented by a cantilever beam, is subjected to resonant harmonic vibrations. Using a measurement setup consisting mainly of a laser sensor and a data

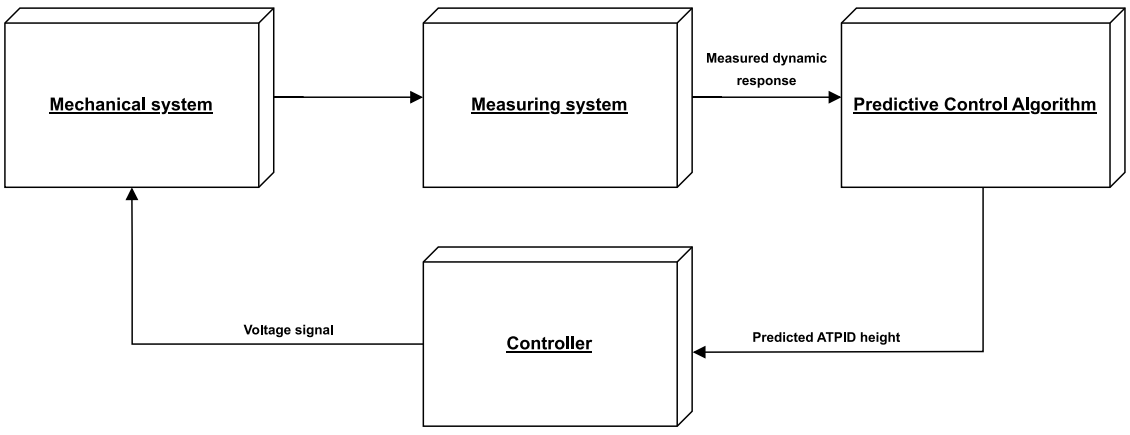

Fig. 7. Scheme of the PCA algorithm implementation for the unknown mechanical system.

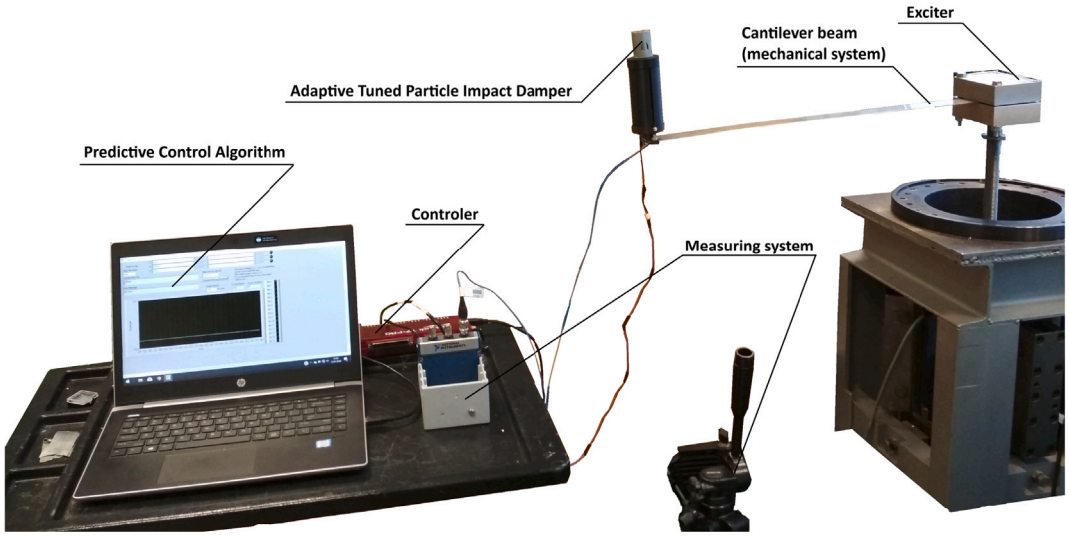

Fig. 8. Experimental test stand.

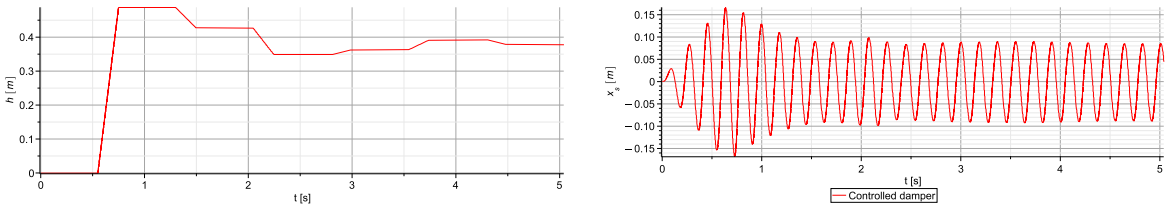

(a) ATPID damper height (b) Displacement of the free end cantilever beam

Fig. 9. Result of the experimental implementation of the PCA algorithm in the unknown mechanical system.

acquisition card, the dynamic response of the system (displacement of the free beam end) is measured. The acquired data is saved on a computer's disk and transmitted to the Predictive Control Algorithm. The test stand is presented in Fig. 8.

Within the Predictive Control Algorithm, the velocity of the grain is estimated using Eq. (16), and the height of the damper is calculated using Eq. (15). Amplitude of the free beam end A_{pred} is achieved by measuring system. The calculated predicted damper height h_{pred} is then sent to the control system, which, in the subsequent stage, generates an appropriate voltage signal for the ATPID damper's electric engine. This process adjusts the container height at the computed value. The delay of the control system is considered by accounting for the following three components: (i) measurement time, (ii) optimal height computation time, and (iii) optimal height setting time. The system's dynamic response measurements are conducted over three subsequent periods of vibration in order to identify maximum amplitude of vibrations and compute velocity of the grain. Thus, the measurement time is given by $t_m = n/f$, where $n = 3$ and f is the vibration frequency, which depends on the mass of the applied grain. The optimal container height is computed using the Predictive Control Algorithm based on the previously determined quantities. Due to the algorithm's computational efficiency, this step typically requires only milliseconds and is negligible compared to the total control delay. Finally, the transition of the container's height from the actual value to the determined optimal one is assumed to take 0.3 [s], as determined by the operational speed of the applied electric engine. Notably, after setting the optimal height, the system remains in a transient state which lasts for substantial period (significantly longer than the control system delay), until the steady state is achieved. The entire process is repeated multiple times until an optimally damped vibration state is achieved. Several test cases were conducted, varying the excitation amplitude and the grain mass. For the sake of clarity, the results of one selected case (where the amplitude of excitation was $A = 0.01$ [m] and grain mass was equal 20% mass of the whole system $m_g = 0.2M$) are presented in Figs. 9 and 10.

According to the earlier description and assumptions, measurements from every consecutive three vibration periods were subjected to analysis, the damper height was calculated, and then applied in the actual ATPID damper. As a result, a time history of the damper control for the entire procedure was obtained and presented in Fig. 9(a). As can be seen, for the presented case, it was necessary to determine several intermediate heights in order to establish the final optimal one. Additionally, it can be observed that the first determined height (excluding the case when the damper is closed) is too large. At a later stage, there were minor oscillations in the predicted height values around the optimal height. The described geometric changes in the container naturally affected the grain motion and the response of the cantilever beam vibrations. The time plot of the vibration amplitude of the free end beam is presented in Fig. 9(b). It can be observed that at the beginning of the measurements, until approximately 0.5 [s], the

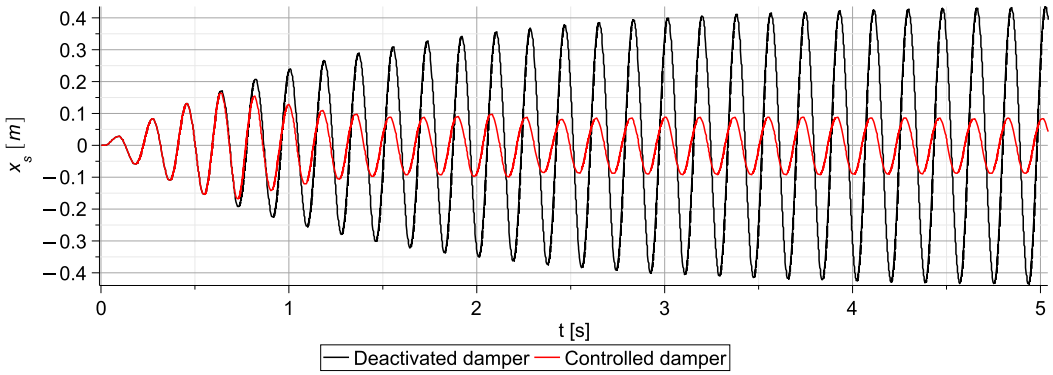

Fig. 10. Comparison of the displacement of the free end of cantilever beam for the case with deactivated and controlled ATPID Damper (case 1).

damper was closed, and gradual increase of the resonant vibrations was observed. Each subsequent opening of the damper resulted in a reduction in the beam vibration amplitude. Ultimately, applying the PCA algorithm allowed to achieve stabilized vibrations with an amplitude below 0.1 [m].

To determine the effectiveness of vibration damping, these results were compared with an analogous case in which the damper height remains minimal throughout the resonant vibration process, which means that no additional damping from the ATPID damper is introduced. The comparison of both results is presented in Fig. 10.

In the situation where the damper is closed, and the grain does not move in the container, full excitation of the beam into resonant vibrations can be observed. Such an example is presented in Fig. 10 by black line. The resonant vibrations are stabilized and reach an amplitude of approximately 0.4 [m]. The response of the beam vibrations with the application of the PCA algorithm is shown by red line. Stabilized and optimally damped vibrations are achieved after around 2 [s] of the experiment. Additionally, it should be noted that the application of the PCA algorithm allows for determining the damper height at which the beam vibration response amplitude is reduced by nearly 75%. These results indicate that PCA is a fast and efficient control algorithm, suitable for systems whose mechanical characteristics are a priori unknown.

To demonstrate the effectiveness of the PCA algorithm, two additional experimental studies were conducted. In the first study (case 2), the amplitude of excitation was set to $A = 0.01$ [m] and grain mass was $m_g = 0.1M$. In the second study (case 3), the excitation amplitude was increased to $A = 0.02$ [m] and the grain mass was $m_g = 0.2M$. The plots illustrate the height of the ATPID damper as well as the oscillation response of the system for both cases: with the damper deactivated and with control applied via the PCA algorithm. The results for each scenario are presented in Figs. 11 and 12.

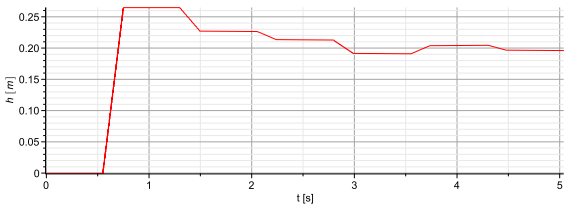

(a) ATPID damper height

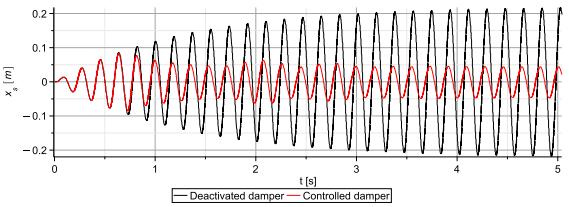

(b) Comparison of the displacement of the free end of cantilever beam for the case with deactivated and controlled ATPID Damper

Fig. 11. Result of the experimental implementation of the PCA algorithm in the unknown mechanical system (Case 2).

The results indicate that the PCA algorithm is applicable to various cases involving changes in excitation amplitude and granular mass. In both scenarios, the algorithm converged within a few iterations to an optimal height at which substantial resonant vibration damping was achieved. In both cases considered, the optimal damper height was approximately 0.2 [m]. Under steady-state conditions, the amplitude of the vibration response was reduced by up to 80% compared to the system with an inactive damper. This PCA-based approach shows potential for vibration suppression in systems with limited prior information. However, a notable disadvantage of this method is a relatively long time required to iteratively determine and adjust the damper height. Longer periods of resonant vibrations can destroy the structure. Consequently, further investigation was undertaken to enable the immediate determination of an optimal damper height, aiming to enhance the efficiency of mechanical vibration reduction at the initial stages of the process.

Parameters such as beam mass, granulate mass, and excitation amplitude also affect the effectiveness of vibration damping. The experimentally obtained effectiveness can be improved, but significant reconstruction of the experimental setup is required, which poses a serious limitation in further experimental research. Therefore, in the subsequent part of the study, the focus was on applying

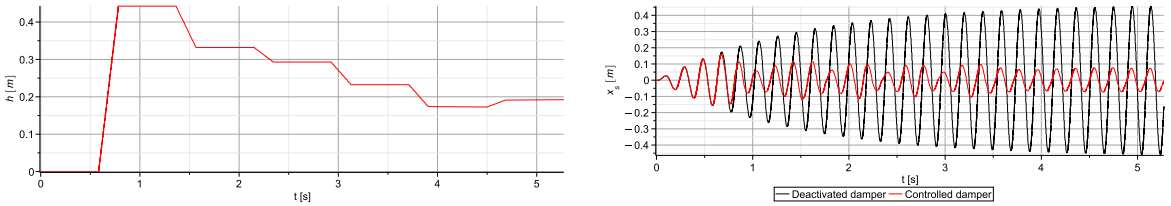

(a) ATPID damper height

(b) Comparison of the displacement of the free end of cantilever beam for the case with deactivated and controlled ATPID Damper

Fig. 12. Result of the experimental implementation of the PCA algorithm in the unknown mechanical system (Case 3).

the PCA algorithm to systems that can be theoretically modeled and system dynamics potentially predicted without the need for experimental investigation.

3. The approach of the PCA implementation for the well-known mechanical system

The second scenario considered in the manuscript assumes that the studied object is well-known and dynamic response of the system at the test stand can be reflected using numerical models. Consequently, it is possible to predict the system's behavior at the initial stage of the algorithm's operation and thus to improve the process of searching for the optimal height of the damper. Additionally, all subsequent steps of the control algorithm are carried out numerically, so the height determination time depends almost exclusively on the computational power of the computer.

Before starting to implement Predictive Control Algorithm the following assumptions have to be provided:

- the excitation parameters (amplitude and frequency) are known,
- the physical and geometric parameters of the beam and ATPID damper are known,
- the ATPID damper is deactivated at the start of the process (the grain is blocked),
- the beam is in resonance during vibrations with the closed ATPID damper.

The implementation scheme of the PCA algorithm is presented in Fig. 13.

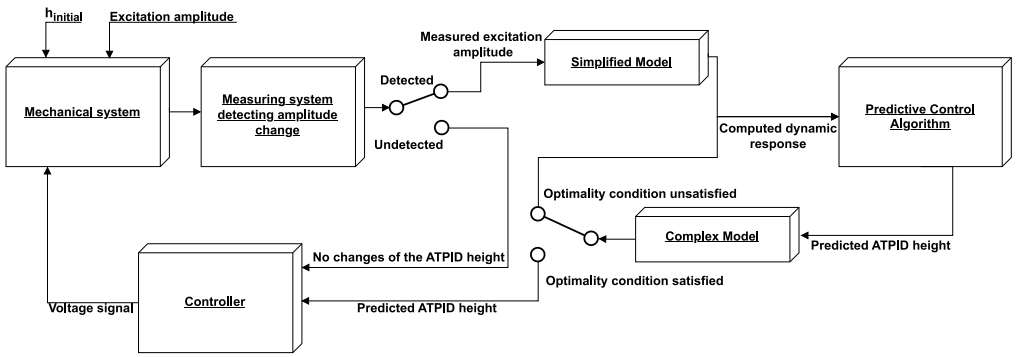

Fig. 13. Scheme of the PCA algorithm implementation for the well-known mechanical system.

The experimental mechanical system consists of a cantilever beam subjected to harmonic kinematic excitation. The ATPID damper is attached to the free end of the beam and is controlled via the PCA algorithm. The amplitude of the excitation may vary over time, while the selected excitation frequency consistently induces resonant vibrations when the damper is deactivated. In the initial phase of the PCA algorithm's operation, the damper is deactivated, meaning its height, denoted as h_{initial}, is equal to the diameter of the sphere placed inside the damper container. For the purposes of the presented study, $h_{\text{initial}} = 0.017$ [m]. During the experimental investigations, the measurement system records the dynamic response of the beam's free end along with the excitation amplitude. At this stage, detection of changes in excitation amplitude is performed. At the beginning of the experiment and at each subsequent stage, whenever a new excitation amplitude is identified, the measured value of the amplitude is transmitted to the PCA algorithm. Based on this input, a simplified model predicts the approximate amplitude of the system's response under the current conditions. This predicted response is forwarded to the Predictive Control Algorithm block, which initiates further processing. The PCA block determines a predicted damper height, which is then passed to a second component — the Complex Model. This model continues the simulation of the system's behavior and verifies whether the proposed damper height meets the criteria for optimal granular

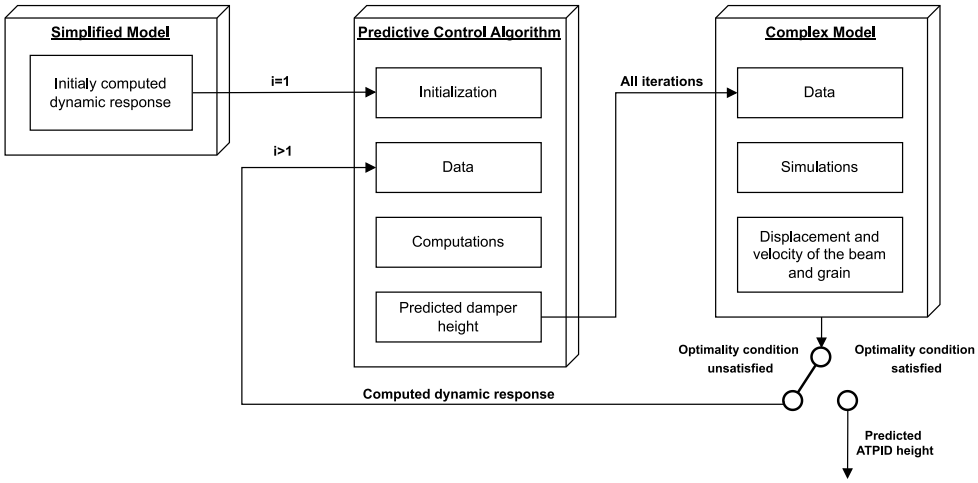

Fig. 14. Optimality condition for the Predictive Control Algorithm.

movement. If the conditions are not satisfied, the Complex Model updates the dynamic response, and a new predicted damper height is computed by the PCA block. In cases where the conditions are satisfied, the computed height is deemed optimal and transmitted to the controller. Each time a new excitation amplitude occurs, it is immediately detected, and the entire PCA algorithm procedure is re-executed to determine the optimal damper height for the current excitation. Until a new optimal value is determined, the previously computed damper height remains applied in the real system. Conversely, when the measurement system does not detect a change in the excitation amplitude, appropriate information is sent to the controller indicating that no adjustment to the damper height is necessary.

The application of the Simplified Model and Complex Model reduces the time required to identify the amplitudes of the system's resonant vibrations in a steady state, significantly accelerating the determination of the optimal damper height. A detailed schematic of the control process using the Simplified Model, Predictive Control Algorithm and Complex Model is presented in Fig. 14 and described in details in the next subsections of the paper.

3.1. Operating principle of the PCA algorithm for the well-known mechanical system

Starting from a Simplified Model (SM), it is possible to predict the system response in the specific case corresponding to damper height greater than the optimal one. Based on the obtained results and the previously defined PCA criteria, the initial value of the damper's height (the first prediction) can be determined using the Predictive Control Algorithm. In the first iteration of the calculations, this value differs from the optimal one because of the application of the Simplified Model containing significant simplifications and aimed primarily at predicting the system response in the range of vibrations when the ATPID damper height is too large. Although the obtained damper height is not optimal, it constitutes the starting point for further calculations, which introduce additional physical phenomena. The following stage utilizes both the Complex Model (CM_i) and the Predictive Control Algorithm (PCA_i) where i enumerates iterations of the PCA algorithm. The Complex Model is the 2-DOF soft contact model that was used in the published paper [52]. These models determine the dynamics of the system and the height of the damper respectively, and exchange data with each other. Iterative running of the Complex Model and Predictive Control Algorithm allows to determine a damper height that is close to the optimal one. Finally, in order to find the height which is the most efficient, a searching process in the range close to the final height is performed. The Simplified Model and the Complex Model are described in detail below. Schemes of the discussed models are shown in Fig. 15.

3.2. Simplified model

The Simplified Model allows studying a specific type of vibration, which occurs when the system's mass consists solely of the beam mass. In this case, the mass of the grain can be omitted, assuming that the contact between the grain and the container walls is infrequent and short. This condition is met when the damper's height is significantly greater than the optimal height, preventing the grain from reaching the upper wall position.

Finding a solution for such a scenario is crucial for determining the expected height of the damper. Therefore, an attempt was made to derive an analytical solution, which will later serve as a component of the Predictive Control Algorithm. For the sake of further analysis, the analytical solution of the Simplified Model is denoted as the predictive solution of the vibrating system x^s_{pred}. It describes oscillations around the equilibrium state, considering the initial deflection $x^s_{pred}(t=0) = -(m_s g)/k_s$ that accounts for the

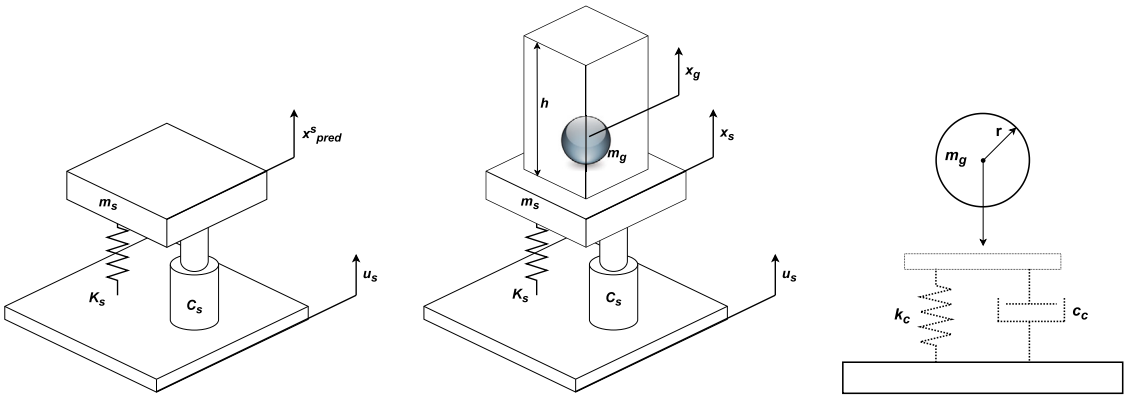

(a) Scheme of the Simplified Model (b) Scheme of the Complex Model (c) Scheme of the contact between grain and wall

Fig. 15. Schemes of the models used in the PCA algorithm.

effect of gravity. Hence, the equation of motion can be represented as a system that does not include the component related to the force of gravity. The initial velocity is $\dot{x}^s_{pred}(t=0)=0$. The equation of motion is defined as:

$$m_s\ddot{x}^s_{pred} + c_s[\dot{x}^s_{pred} - \dot{u}_s] + k_s[x^s_{pred} - u_s] = 0 \tag{17}$$

The kinematic excitation takes the harmonic form $u_s = Asin(2\pi ft)$ and then the Eq. (17) reads:

$$m_s\ddot{x}^s_{pred} + c_s\dot{x}^s_{pred} + k_s x^s_{pred} = D_{red}sin(2\pi ft) \tag{18}$$

where the excitation frequency and natural frequency of the system are presented by Eqs. (19) and (20), respectively:

$$f = \frac{\sqrt{k_s}}{2\pi\sqrt{m_s + m_g}} \tag{19}$$

$$f_0 = \frac{\sqrt{k_s}}{2\pi\sqrt{m_s}} \tag{20}$$

Using basic theory from the field of mechanical vibrations, a detailed formula to calculate the reduced amplitude of a harmonic force excitation can be derived:

$$D_{red} = \sqrt{A_0^2 + B_0^2} \tag{21}$$

where: $A_0 = k_s A$, $B_0 = c_s \omega A$ and $\omega = 2\pi f$.

The steady state system response takes the form of a trigonometric function:

$$x^s_{pred} = A_{pred}sin(2\pi ft) \tag{22}$$

where the amplitude of vibrations can be calculated by Eq. (23):

$$A_{pred} = \frac{D_{red}}{m_s\sqrt{4\beta^2\omega^2 + (\omega^2 - \omega_0^2)^2}} \tag{23}$$

and $\omega_0 = 2\pi f_0$.

In summary, x^s_{pred} is the displacement of the system, which has a mass equal to the mass of the beam. The frequency of excitation is calculated based on both the mass and the beam. The analytical solution is computed for the case where the parameters are as follows: $m_s = 0.3258$ [kg], $m_g = 0.1M_s = 0.0362$ [kg] where is the whole mass of the 2-DOF system, $k_s = 427.6$ [$\frac{\mathrm{N}}{\mathrm{m}}$], $c_s = 0.56$ [$\frac{\mathrm{N\ s}}{\mathrm{m}}$], $A = 0.02$ [m], $f = 5.469$ [Hz], $f_0 = 5.765$ [Hz]. In order to verify the above result the 2-DOF soft contact model was applied and the damper height was set significantly larger than the optimal one such that the grain could not collide with the container ceiling. The steady-state solution obtained from the Simplified Model and the numerical simulation of the mentioned 2-DOF model are compared and presented in Fig. 16.

The results indicate that the vibration amplitude determined from the analytical model closely matches the mean maximum amplitude of the successive vibration periods obtained from the 2-DOF model. It is evident that slight phenomena of rumble can also be observed. This is due to the fact that a significantly larger height than optimal was applied in the model. The occurrence of rumble phenomena in such situations is often. This means that the Simplified Model can be used for preliminary prediction of the dynamics of the beam equipped with the ATPID damper with a height larger than optimal. This stage is crucial for further PCA algorithm procedures as it provides the preliminary vibration prediction of the system in the above specific state.

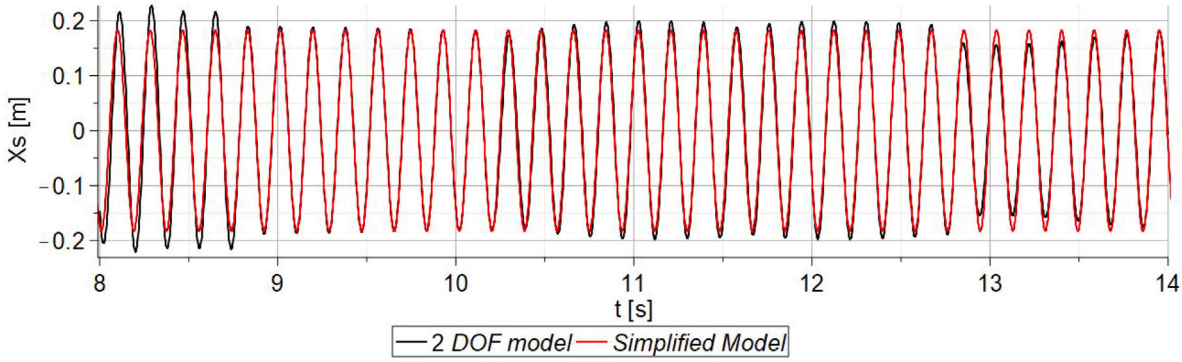

Fig. 16. Comparison of the response of the beam vibration obtained from the Simplified Model — red line (when $M_s = m_s$) and the 2-DOF soft contact model — black line (when the damper height exceeds the optimal height).

3.3. Complex model

The scheme of the Complex Model is presented in Fig. 15(b) and its governing equations are given by Eqs. (24) and (25):

$$m_s\ddot{x}_s + k_s[x_s - u_s] + c_s[\dot{x}_s - \dot{u}_s] + m_s g + F_{c_1} - F_{c_2} = 0 \tag{24}$$

$$m_g\ddot{x}_g + m_g g - F_{c_1} + F_{c_2} = 0 \tag{25}$$

The kinematic excitation applied to the system is characterized by a function that describes the motion of the structure support, as expressed by the equation below:

$$u_s = Asin(2\pi f t) \tag{26}$$

where the excitation frequency has the following form:

$$f = \frac{\sqrt{k_s}}{2\pi\sqrt{m_s + m_g}} \tag{27}$$

To model the collision phenomena, the soft contact theory was employed. This approach enables a detailed numerical analysis by assuming that the time of contact between two objects is very short and finite, in contrast to the hard contact theory, which presumes an infinitely short collision. An additional advantage of this model is its ability to account for elastic and viscoelastic properties of the colliding objects [66]. A detailed description and analysis of the chosen contact force model are presented in the previously published paper [52]. The nonlinear viscoelastic lower F_{c_1} and upper F_{c_2} contact forces can be computed by Eqs. (28) and (29):

$$F_{c_1} = k_c\xi_{c_1}^{3/2} + c_c\dot{\xi}_{c_1}\xi_{c_1}^{1/4} \tag{28}$$

$$F_{c_2} = k_c\xi_{c_2}^{3/2} + c_c\dot{\xi}_{c_2}\xi_{c_2}^{1/4} \tag{29}$$

where $k_c = (4/3)E_{eff}\sqrt{r}$ and $c_c = 2\sqrt{k_c m_g}$ describe the reduced contact stiffness and damping, respectively. Both coefficients depend on the grain radius r and the effective Young modulus $1/E_{eff} = (1-\nu_w^2)/E_w + (1-\nu_g^2)/E_g$, where Poisson's ratios of the wall and grain are denoted by ν_w and ν_g, while Young's moduli of the wall and grain are represented by E_w and E_g, respectively.

Contact forces depend on the overlaps (ξ_{c_1}, ξ_{c_2}) and overlaps rates ($\dot{\xi}_{c_1}$, $\dot{\xi}_{c_2}$). To calculate these parameters it is necessary to introduce the equations defining the distance between the grain and the floor (τ_{c_1}) and the ceiling (τ_{c_2}) of the container:

$$\tau_{c_1} = -x_{g_i} + r + x_s - x_g \tag{30}$$

$$\tau_{c_2} = x_{g_i} + r + x_g - x_s - h \tag{31}$$

where $x_{g_i} = r$. The overlaps and overlaps rates have the following forms:

$$\xi_{c_1} = \begin{cases} \tau_{c_1} & \text{if } \tau_{c_1} > 0 \\ 0 & \text{if } \tau_{c_1} \le 0 \end{cases} \tag{32}$$

$$\xi_{c_2} = \begin{cases} \tau_{c_2} & \text{if } \tau_{c_2} > 0 \\ 0 & \text{if } \tau_{c_2} \le 0 \end{cases} \tag{33}$$

$$\dot{\xi}_{c_1} = \begin{cases} \dot{x}_s - \dot{x}_g & \text{if } \xi_{c_1} > 0 \\ 0 & \text{if } \xi_{c_1} = 0 \end{cases} \tag{34}$$

$$\dot{\xi}_{c_2} = \begin{cases} \dot{x}_g - \dot{x}_s - \dot{h} & \text{if } \xi_{c_2} > 0 \\ 0 & \text{if } \xi_{c_2} = 0 \end{cases} \tag{35}$$

Due to the nature of the central collision between the grain and the wall (where the directions of motion of the grain and the wall is the same), friction during contact was neglected. A similar approach was adopted in the paper [67].

In the ATPID damper the height of the container is tunable. It means it can be changed in real time. The ATPID height can be expressed by Eq. (36):

$$h = h_{old} + \Delta h \psi \tag{36}$$

$$\Delta h = h_{max} - h_{old} \tag{37}$$

where h_{max} in the new predicted damper height, h_{old} is the container height computed in the last iteration of calculations. The damper height can be tuned from the value h_{old} to the h_{max}. The function of these changes can be described by the control function ψ which corresponds to the linear changes generated by the electric engine of the ATPID damper and has the following form:

$$\psi = \begin{cases} 0 & \text{if } t < t_1 \\ \frac{t - t_1}{\Delta t_{12}} & \text{if } t_1 < t < t_2 \\ 1 & \text{if } t > t_2 \end{cases} \tag{38}$$

where: t — control time, t_1 — activation start time, t_2 — saturation start time, t_{12} — activation period.

The initial conditions $x_s(t = 0)$, $x_g(t = 0)$, $\dot{x}_s(t = 0)$ and $\dot{x}_g(t = 0)$ of each simulation depend on the final conditions of the previously completed numerical simulation. Therefore, they will be different each time and enable the continuation of previous analyses with the consideration of newly determined damper heights.

3.4. Application of the simplified model and predictive control algorithm

The first step of calculations was the application of Simplified Model and Predictive Control Algorithm to determine h_{pred} for the excitation amplitude $A = 0.02$ [m]. The preliminary predicted height is determined and equals $h_{pred} = 0.549$ [m]. At this stage, it is worth examining how the dynamic response of the tested system changes for the specified damper height. For this purpose, the Complex Model can be treated as a universal 2-DOF soft contact model for the experimental system under study. Accordingly, the determined height was included in the such 2-DOF model and a numerical simulation was performed. The response of the system was presented in Fig. 17.

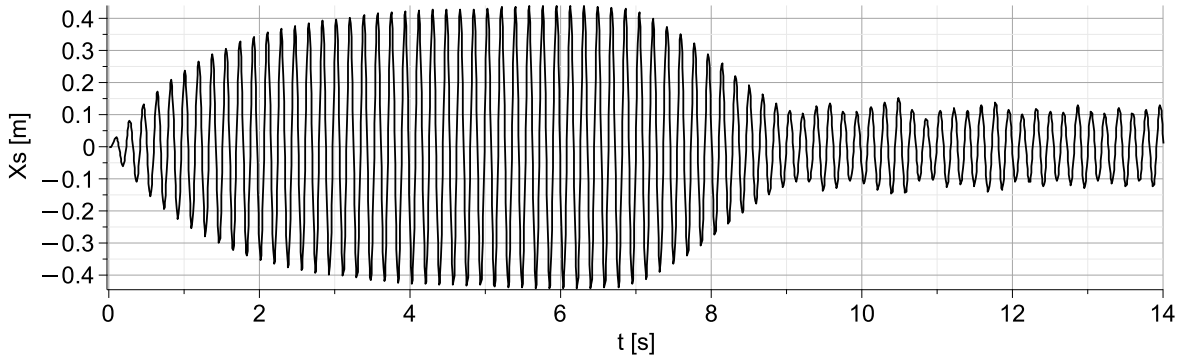

Fig. 17. Response of the beam vibrations for 2-DOF soft contact model with initially predicted ATPID height for excitation amplitude $A = 0.02$ [m].

Upon analyzing the results, it becomes evident that the initially determined height is larger than the optimal one, and there is a rumble effect observed in the vibrations of the beam. Once the specified height h_{pred} is set, the system starts to vibrate in a chaotic manner due to the irregular movement of the grain within the container. This confirms that the SM allows for predicting the response amplitude of the system for damper heights larger than the optimal height, while the PCA enables determining the height at which this situation occurs. Additional analysis will be conducted to further tune this height of the damper, ensuring that the particle movement meets the predetermined criteria.

The displacement of the bottom wall of the container is determined using the analytical solution x^s_{pred} obtained from the Simplified Model (Eq. (22)), while the displacement of the upper wall of the container can be calculated as the sum of the displacement of the floor and the predetermined height of the damper (Eq. (7)). Based on the initial velocity of the grain $V_{grain} = V_{beam} = 6.24$ [m/s], its movement towards the damper ceiling can be determined. The subsequent collision with the upper wall of the damper occurs when the position of the beam reaches zero (at its maximum velocity). It was assumed that each simulation iteration should begin from a similar situation — the moment when the grain collides with the bottom wall of the casing. Therefore,

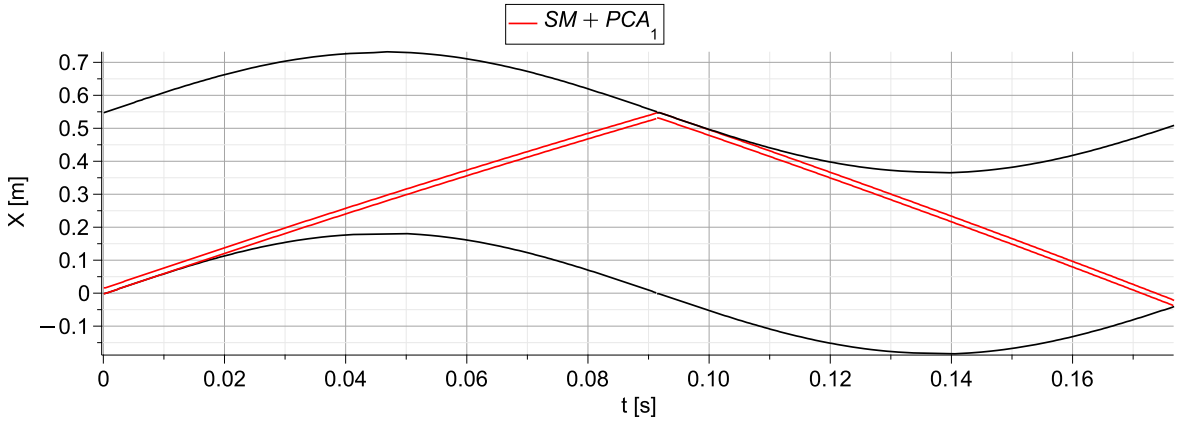

Fig. 18. Upward and downward motion of the grain in the container computed using Simplified Model with initially predicted heigh h_{pred} obtained from the Predictive Control Algorithm.

to proceed to the next analysis, the grain's subsequent trajectory was calculated. After contacting the upper wall, the velocity of the particle was assumed to be equal to the velocity of the beam before the collision, similarly as at the beginning of the simulation. Consequently, the displacement of the grain while moving downward was determined. The obtained results are presented in Fig. 18.

Subsequently, the time at which the grain collided again with the bottom wall of the damper was determined. At the moment of collision, the position and velocity of the beam and the particle were $X_{beam} = -0.0382$ [m], $X_{grain} = -0.0297$ [m], $V_{beam} = 6.136$ [m/s] and $V_{grain} = -6.972$ [m/s], respectively. These values serve as the initial conditions for the simulation, which will be continued in the Complex Model.

3.5. Application of the Complex Model and Predictive Control Algorithm

The Complex Model is a 2-DOF soft contact model that incorporates more physical phenomena, including grain-walls collisions, compared to the Simplified Model. The CM allows observation of the system's dynamic response to the grain's motion and the resulting collisions over subsequent vibration cycles. It is assumed that each simulation based on the Complex Model lasts 5 s. Starting from the previously computed initial conditions and the primary height of the damper obtained from the Predictive Control Algorithm (PCA_1), the simulation was further conducted using the Complex Model (CM_1). The results of this simulation are presented in Fig. 19.

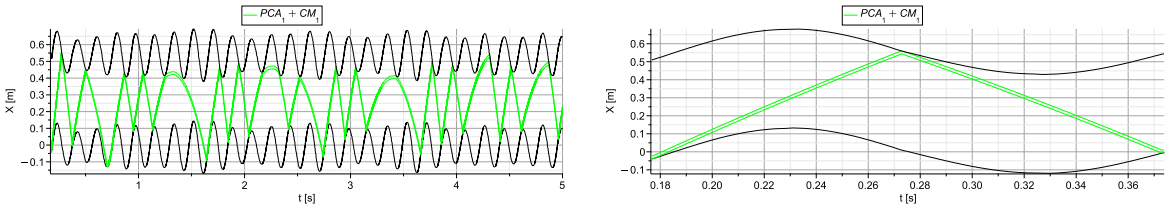

(a) General movement (b) Detailed movement

Fig. 19. Movement of the grain and container walls obtained from the Complex Model.

The grain motion during the current simulation is analyzed to verify whether the damper height determined in PCA_1 results in optimal grain behavior. For the case shown in Fig. 19(a), it can be seen that the grain motion is not predictable. Random collisions occur, and the criteria for optimal grain motion are not satisfied. In such cases, it is assumed that only the grain motion during the first vibration cycle will be considered for further analysis, as illustrated in Fig. 19(b).

Concluding, the entire movement of the particle and the damper walls can be traced from the beginning of the Predictive Control Algorithm process, where the initial system response and damper height were determined. Specifically, the first cycle of upward and downward movement of the grain and the damper can be computed using the Simplified Model and the Predictive Control Algorithm ($SM + PCA_1$). The second cycle of upward and downward movement of the grain can be computed for the previously determined damper height using the Predictive Control Algorithm and the Complex Model ($PCA_1 + CM_1$), considering collisions described by the soft contact theory. At the end of the last impact with lower wall (Fig. 19(b)), the position and velocity of the beam and the grain are as follows: $X_{beam} = -0.0029$ [m], $X_{grain} = 0.0056$ [m], $V_{beam} = 2.689$ [m/s], $V_{grain} = 4.114$ [m/s]. These values will be considered as input data for further calculations in the Predictive Control Algorithm.

Then, the second iteration of the PCA algorithm begins to determine the new height of the damper. The general form of Eq. (14) is used. For a clearer representation of the subsequent mathematical operations, the formula is restated below:

$$h_{pred} = 2r + X_{beam} + V_{grain}(t_{c2} - t_{c1}) - \frac{g(t_{c2} - t_{c1})^2}{2} - A_{pred} sin(2\pi f t_{c2}) \tag{39}$$

The times t_{c1} and t_{c2} represent the time of contact between the grain and the lower and upper walls of the damper, respectively, based on the predicted system response A_{pred}. The time t_{c1} needs to be determined by solving Eq. (40):

$$A_{pred} sin(2\pi f t_{c1}) = X_{beam} \tag{40}$$

The equation above has multiple solutions, and the time t_{c1} can take various values. However, for subsequent calculations, we consider the value that falls within the first period of vibrations. To fulfill the assumption that the grain must collide with the ceiling of the damper when it reaches its maximum velocity, the time t_{c2} needs to be equal to $1/(2f)$. For the updated parameters, it is possible to re-determine the predicted height using the Predictive Control Algorithm (PCA_2), apply it to the Complex Model (CM_2) and continue the simulation determining the vibration of the beam and the movement of the grain. The results obtained for the next iteration of the calculations are presented in Fig. 20.

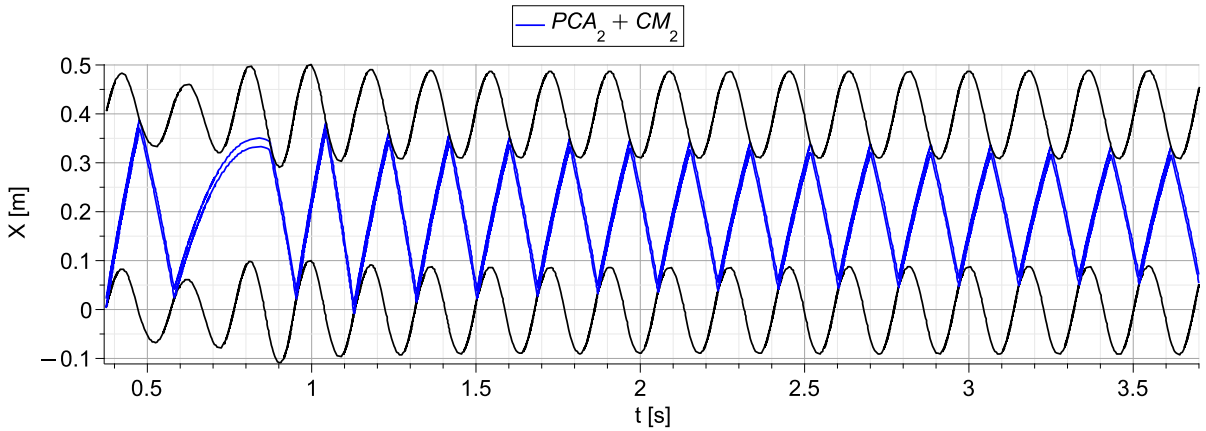

Fig. 20. Motion of the grain and container for the new predicted damper height.

Upon analyzing the results, it becomes evident that collisions between the particle and the container occur periodically when the direction of the grain is opposite to the direction of the damper movement, the beam velocity is close to its maximum, and there is no sticking effect between the grain and the cylinder walls. These conditions indicate that all the criteria for optimal grain movement are met. The entire movement of the particle within the container, controlled by the entire PCA algorithm, is depicted in Fig. 21.

The height obtained using the PCA algorithm, referred to as the predicted optimal height, is the final value after considering all the assumed conditions and in this case is equal 0.3922 [m].

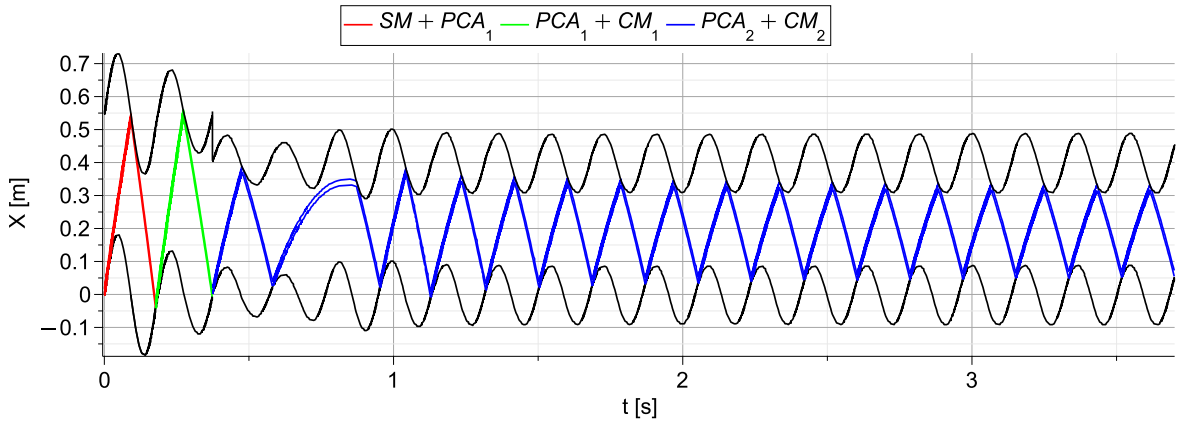

Fig. 21. Motion of the grain and damper walls from the beginning of the calculations.

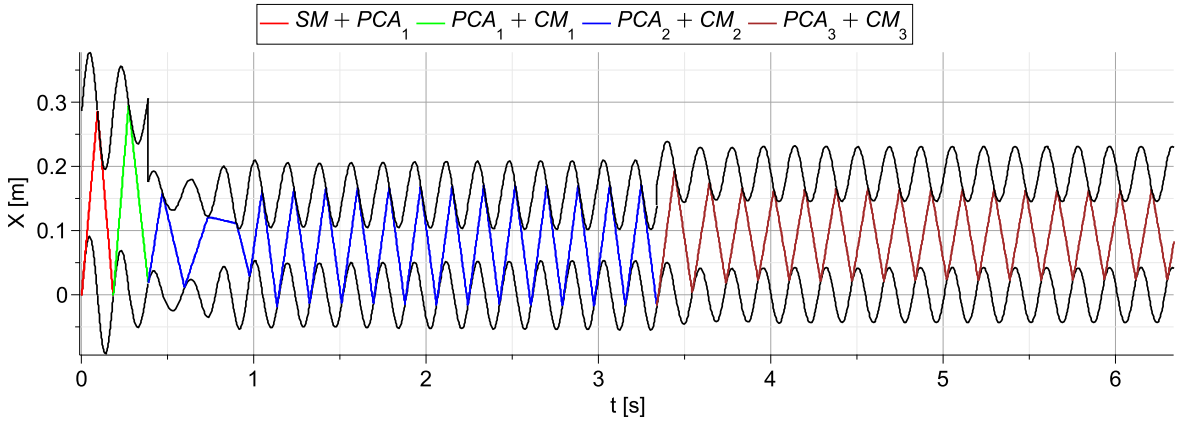

Fig. 22. Motion of the grain and damper walls from the beginning of the calculations (case 2).

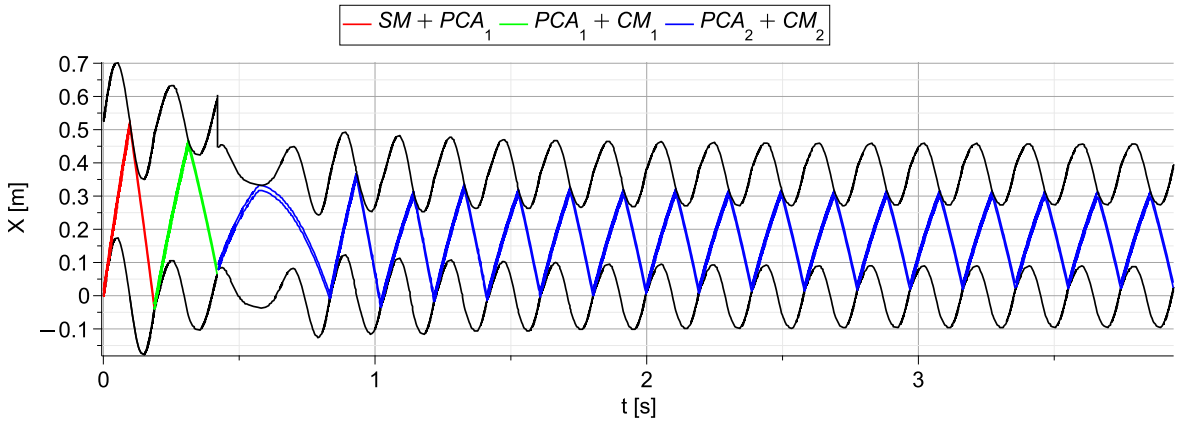

Fig. 23. Motion of the grain and damper walls from the beginning of the calculations (case 3).

For the above approach, two additional cases were considered: in Case 2, the excitation amplitude was $A = 0.01$ m with $m_g = 0.2$ M and in Case 3, $A = 0.02$ [m] with $m_g = 0.1$ M. The results for these cases are presented sequentially in Figs. 22 and 23.

The obtained results indicate that for different conditions, it is also possible to determine an final predicted damper height that can be immediately implemented in the mechanical system. In the analyzed cases, the optimal damper height was 0.205 [m] for case 2 and 0.198 [m] for case 3, aligning with the findings from the section on applying PCA in an unknown system. Additionally, it was observed that in the scenario with a lower excitation amplitude (Fig. 22), achieving the height at which optimal granular motion criteria are met required three iterations of calculations using the Complex Model. For Case 3, only two iterations were necessary. It is crucial to ensure that these initially determined damper heights are indeed the optimal one, which means that it minimizes the amplitude of the beam's vibration. To achieve this, it is necessary to explore a range of values around the last predicted height and determine the container height that results in the optimal system response.

3.6. Precise tuning of pre-determined ATPID height

The searching process constitutes the final stage in determining the optimal ATPID height. It is an iterative method in which various damper heights are evaluated and the corresponding system responses are compared, including the maximum amplitude observed in the last two vibration periods (of the simulation). The results of each iteration are assessed relative to the previous ones, allowing for the identification of the most effective damper height at each step. If the response amplitude at the currently tested height is lower than that of the previous iteration, this new height is adopted as the most effective. Otherwise, the damper height from the previous iteration is retained. Fig. 24(a) shows the final heights in each iteration of the precise tuning process (black line), along with all the intermediate height values tested during the process (red points), while Fig. 24(b) presents the amplitude of the system response for the corresponding cases.

The searching process involves gradually decreasing the previously calculated damper height h_{pred} by 10% of its value and observing the changes in the system's response. The system vibration response is analyzed using a 2-DOF soft contact model. This

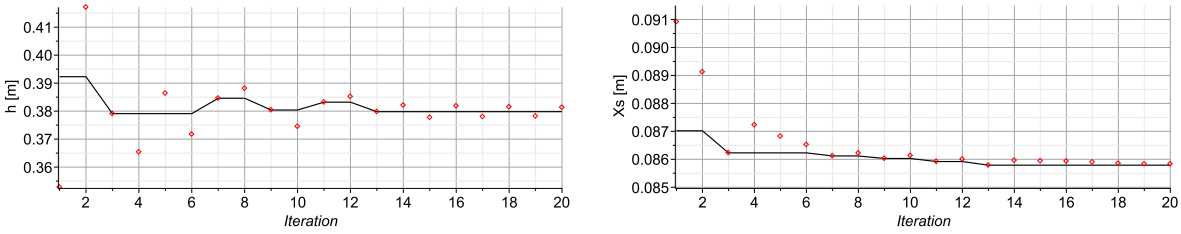

(a) Changes of the ATPID damper height (b) Response of the cantilever beam for the ATPID heights

Fig. 24. ATPID damper heigh and beam response obtained in the searching process (black line) and all tested cases (red points).

height reduction process is repeated until the system's response amplitude starts to increase. The last calculated height (h_{pred}) is then increased by $\frac{h_{pred}\cdot 10\%}{1.5}$, and the response of the beam is analyzed again. This stage continues until the system's response begins to deteriorate which is indicated by an increase in vibration amplitude. The entire procedure is then repeated, and the damper height is modified by $\frac{h_{pred}\cdot 10\%}{1.5n_s}$, where n_s increases by 1 each time the transition from decreasing to increasing the height, or vice versa, is performed. The results obtained from the PCA control algorithm itself are compared with the results from the searching stage. Fig. 24(a) illustrates the process in which the damper height is alternately decreased and increased, allowing for the determination of the optimal height for the specified system parameters. Fig. 24(b) displays the steady-state vibration amplitudes of the system for individual heights evaluated in the search process. There are segments where the height remains constant over selected iterations, for example, iterations 1–2, 3–6, 7–8, 9–10, 11–12, and 13–20. This occurs because, in each iteration, the precise tuning algorithm evaluates the effect of determined damper height on the system's response. Moreover, the vibrations of the beam are consistently reduced throughout the process, indicating the correctness of the algorithm in searching for the optimal height corresponding to the minimum vibration amplitude. In this specific case, it was sufficient to perform 20 iterations of calculations to determine the optimal height of the ATPID damper. In the general scenario, the searching process will continue until successively determined heights will result in changes of vibration amplitude smaller than 1%.

3.7. Final implementation of the PCA algorithm in the real mechanical system

In order to demonstrate the performance of the proposed PCA control algorithm for the ATPID damper connected to a real well-known system, appropriate experimental investigations were conducted. An experimental scenario was proposed in which a cantilever beam, attached to a kinematic exciter, was subjected to three different excitation amplitudes. These amplitudes changed every 5 s and took values of 0.02 [m], 0.01 [m], and 0.015 [m], respectively. The mass of the grain was equal to 10% of the total system mass. With the damper deactivated (i.e., set to its minimal height), the system was subjected to resonant vibrations. The time history of the excitation amplitude is presented in Fig. 25(a). The resulting damper height over time, as determined by the PCA control process, is shown in Fig. 25(b). The vibration response of the free end of the cantilever beam, for both the deactivated and controlled ATPID damper cases, is presented in Fig. 26.

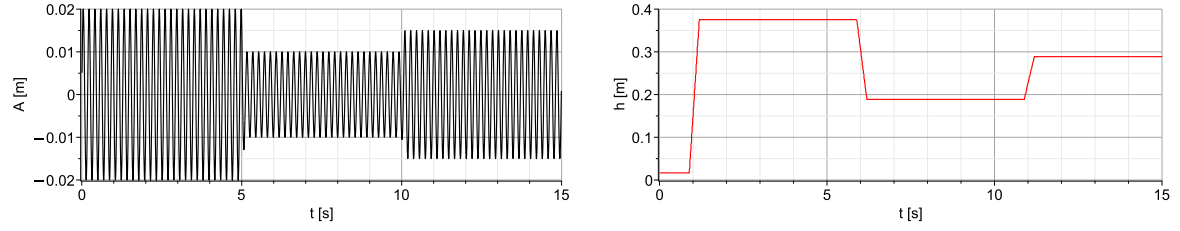

(a) Various excitation amplitude (b) ATPID damper height

Fig. 25. Result of the experimental implementation of the PCA algorithm in the well-unknown mechanical system.

Fig. 26 presents a comparison of the results, from which it can be concluded that the application of the PCA algorithm enables adaptive vibration damping of a beam subjected to excitation of varying amplitude. This approach allows for effective vibration reduction each time the operating conditions change. Based on the conducted analysis, it is observed that the vibration amplitude of the controlled system is reduced by up to approximately 75% compared to the system with the deactivated damper. An analysis of Fig. 25(b) reveals how the damper height changes over time, representing an adaptive response to the varying excitation. It can be observed that there is a certain delay time between the actual change in excitation amplitude and the adjustment to the optimal damper height. This delay is approximately 1.2 [s] and includes the time required to measure a full vibration period and identify the amplitude change (about 0.18 [s]), the computation time of the PCA algorithm with precise tuning process (around 0.7 [s]), and the time needed to adjust the damper height (close to 0.3 [s]). It should also be noted that the time required for

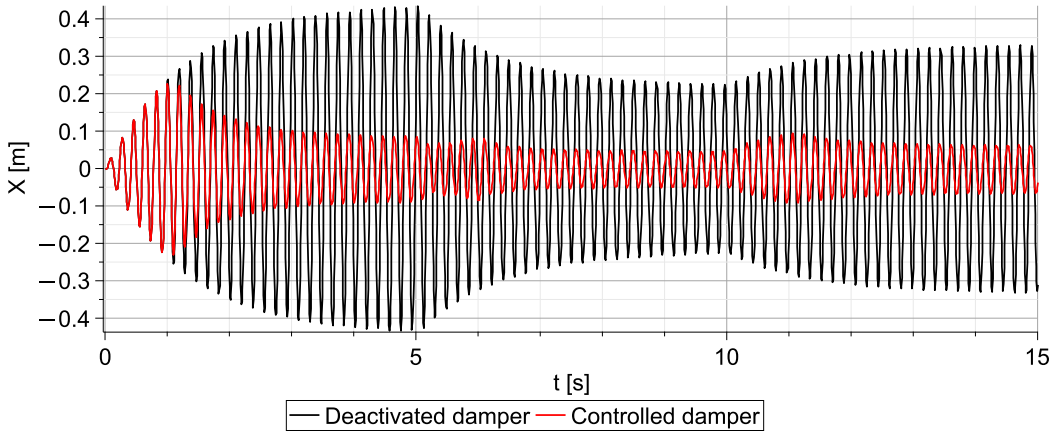

Fig. 26. Comparison of the displacement of the free end of cantilever beam for the case with deactivated and controlled ATPID damper.

the system response to stabilize depends on the parameters of the tested system, which influence the transient response duration after the damper height is adjusted. The obtained reaction time of the PCA algorithm to excitation changes is considered acceptably short. The conducted analysis demonstrates the feasibility of applying the proposed PCA algorithm for vibration control in a real mechanical system subjected to variable operating conditions.

4. Sensitivity analysis of the PCA algorithm

The presented control algorithm allows for determining the predicted height of the damper, which shows that the calculated values are close to the optimal one. To find the final optimal position of the container ceiling, a searching process was applied around the predicted height. As a result, an algorithm was developed that can predict the appropriate height of the ATPID damper for various system parameters, ensuring the most effective reduction of vibrations. Consequently, as a next step, a sensitivity analysis of the proposed Predictive Control Algorithm was conducted.

In the first scenario, optimal damper heights were determined (after using the PCA algorithm and the searching process) for various excitation amplitudes, and the results are illustrated in Fig. 27(a). The remaining system parameters are kept constant and assume the following values: $m_s = 0.905m_b = 0.3258$ [kg], $m_g = 0.1M_s = 0.0362$ [kg], $k_s = 427.6$ [$\frac{\mathrm{N}}{\mathrm{m}}$], $c_s = 0.56$ [$\frac{\mathrm{N\ s}}{\mathrm{m}}$] and $f = 5.469$ [Hz].

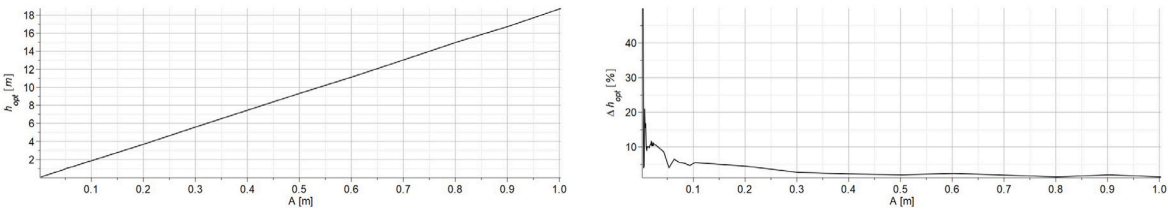

(a) Optimal ATPID damper height (b) Effectiveness of the PCA algorithm

Fig. 27. Change of the optimal ATPID height and effectiveness of the PCA algorithm in terms of various excitation amplitudes.

Based on Fig. 27(a), it can be concluded that the variation of optimal heights over a broad range of excitation amplitudes follows a linear trend. These results are intriguing as the numerical model of the system (Complex Model) is highly nonlinear. Subsequent analyses involved calculating the percentage difference between the preliminary damper height value determined by the PCA algorithm and the final optimal height obtained through the searching process. These results serve as a parameter to evaluate the effectiveness of the proposed PCA algorithm (Fig. 27(b)).

Fig. 27(b) illustrates that the percentage error decreases up to 4% as the excitation amplitude increases. A notable observation is the occurrence of significant percentage discrepancies (ranging from about 10% to 50%) for small amplitudes of excitation (up to approximately 0.1 [m]). These discrepancies appear predominantly due to the influence of gravity on the dynamic response of the system. With small excitation amplitudes, the velocities and accelerations of the vibrating system and grain are relatively small. Consequently, the grain in the open damper remains in constant contact with the floor or achieves only a negligible separation distance when it detaches. In such cases, the correct determination of the damper height using the PCA algorithm while considering all criteria for optimal grain motion becomes challenging. As a result, the discrepancy between the initially determined height and the final optimal height becomes significant.

Next, the optimal heights of the ATPID damper were determined for three grain masses ($m_g = 0.1M_s$, $m_g = 0.2M_s$ and $m_g = 0.3M_s$) while considering a wide range of excitation amplitudes. The results are presented in Fig. 28(a).

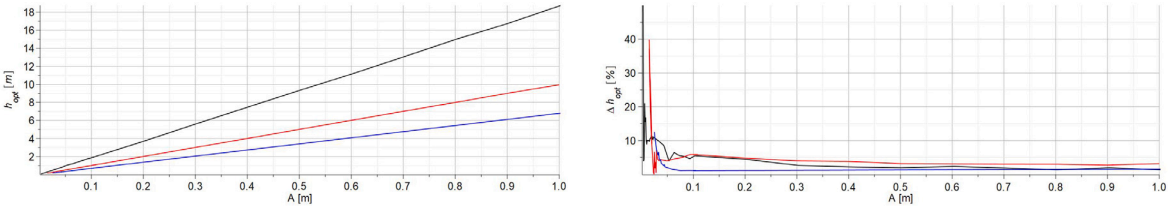

(a) Optimal ATPID damper height (b) Effectiveness of the PCA algorithm

Fig. 28. Change of the optimal ATPID height and effectiveness of the PCA algorithm in terms of the mass of the grain ($m_g = 0.1M_s$ - black line, $m_g = 0.2M_s$ - red line, $m_g = 0.3M_s$ - blue line) for various excitation amplitudes.

The linear relationship between the optimal height of the absorber and the excitation amplitude is observed in all three cases presented in Fig. 28(a). Additionally, the calculations were performed for several grain masses ranging from 10% to 30% of the total system mass. The optimal heights exhibit similar dependencies on the amplitude change and can be precisely approximated by linear regression models, each having different slope parameters for the respective cases. However, to maintain consistency and clarity, these results were not included in the figure.

For the three different cases with various grain masses, the effectiveness of the PCA algorithm was evaluated and the results are displayed in Fig. 28(b). It is evident that the algorithm's efficiency depends on the excitation amplitude also when the grain has different mass. For small excitation amplitudes, the algorithm's performance is relatively low, with differences ranging from 40% to 10%. However, as the amplitude values increase, the error diminishes, and the difference between the initially determined height (from the PCA algorithm) and the height after the search stage reduces to approximately 4%. These values can be considered as an acceptable from a functional point of view. As previously mentioned, the limited effectiveness of the algorithm for small excitation amplitudes can be attributed to the significant influence of gravity on the system's dynamics.

In order to validate this conclusion, optimal damper heights were determined for cases with and without gravity, as well as for various grain masses. The results presented in Fig. 29(a) correspond to a particle with a mass equal to 10% of the total system mass. Additionally, the percentage error, representing the effectiveness of the PCA algorithm, was calculated and shown in Fig. 29(b).

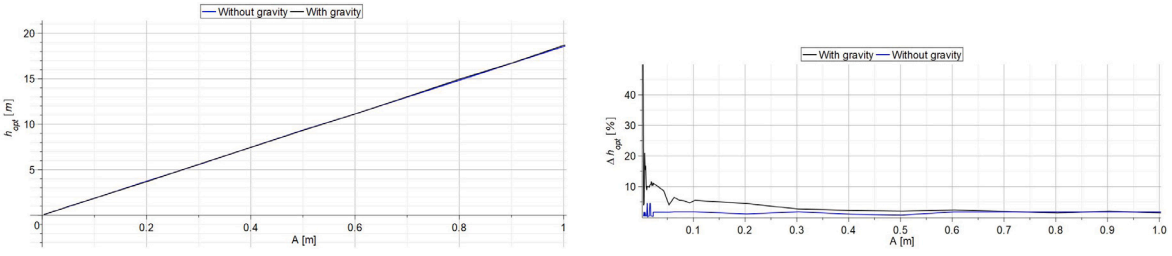

(a) Optimal damper height (b) Effectiveness of the PCA algorithm

Fig. 29. Change of the optimal ATPID height and effectiveness of the PCA algorithm in terms of the various excitation amplitudes for the cases with and without gravity.

Fig. 29(a) illustrates the linear correlation between the optimal height of the ATPID damper for various excitation amplitudes in two distinct scenarios: with and without the gravity. The plots show that the optimal absorber height remains nearly linear for a given amplitude, regardless of whether gravity is considered or not, indicating no significant difference. A more detailed analysis of the impact of gravity is provided by comparing the calculated errors for both cases, as depicted in Fig. 29(b). It turns out that disregarding the phenomenon of gravity makes the PCA algorithm highly effective for the entire considered range of excitation amplitudes. The error between the results is small, and equals approximately 2%. Since both systems (with gravity and without gravity) obtain almost identical optimal heights (Fig. 29(a)), it can be concluded that, to enhance the efficiency of the control algorithm, a model without gravity can be used.

Another interesting problem is to identify the type of function (linear or nonlinear) describing the correlation between the grain masses and the optimal heights. Hence, an analysis was conducted to determine the optimal height of the ATPID damper for four different excitation amplitudes ($A_1 = 0.9$ [m], $A_2 = 0.2$ [m], $A_3 = 0.1$ [m], $A_4 = 0.03$ [m]), considering particle masses ranging from 10% to 30% of the total system mass. The results obtained from this analysis are presented in Fig. 30.

The graphs presented in Fig. 30 reveal a non-linear correlation between the optimal height of the damper and the variation of grain mass, irrespectively of the excitation amplitude. This non-linearity poses a challenge in predicting the system's behavior accurately. As a result, there is a necessity to develop algorithms capable of rapid determination of the optimal damper height for various combinations of excitation amplitudes and particle masses, such as the proposed in the manuscript Predictive Control Algorithm.

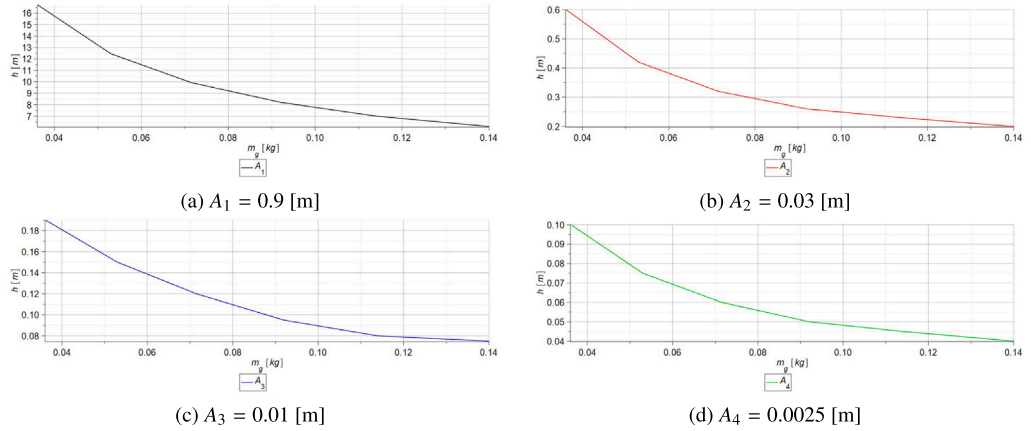

(a) $A_1 = 0.9$ [m] (b) $A_2 = 0.03$ [m]

(c) $A_3 = 0.01$ [m] (d) $A_4 = 0.0025$ [m]

Fig. 30. Change of the optimal ATPID height in terms of the mass of the grain (from 10% to 30% of the mass of the whole system) for various excitation amplitudes.

In the last phase of the investigation, the parameter $d = (X_{ud} - X_{od})/X_{ud} \cdot 100\%$ which represents the percentage ratio of the difference between the amplitude of undamped steady-state vibrations X_{ud} and the optimally damped steady-state vibrations X_{od} to the undamped vibrations. The optimal height required for increasing damper effectiveness was obtained through the proposed PCA algorithm and the searching process. The obtained result is depicted in Fig. 31.

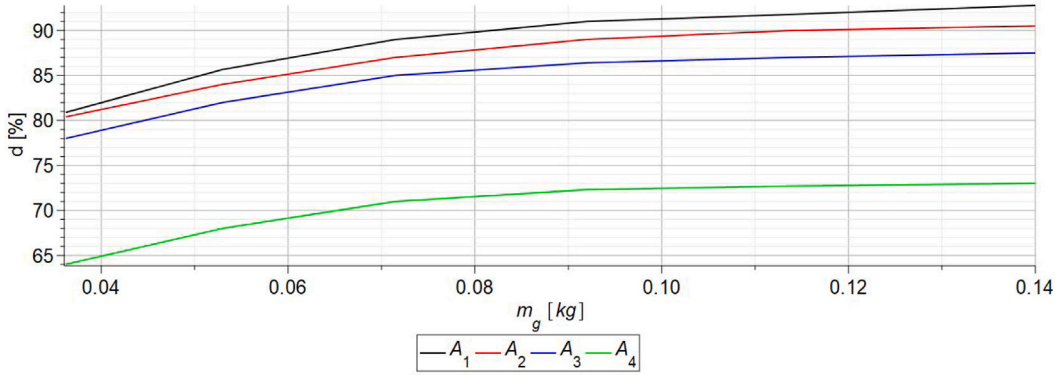

Fig. 31. ATPID damper efficiencies corresponding to optimal container heights for various grain mass and excitation amplitudes ($A_1 = 0.09$ [m], $A_2 = 0.03$ [m], $A_3 = 0.01$ [m], $A_4 = 0.0025$ [m].

Fig. 31 demonstrates that increasing the grain's mass enhances the ATPID damper's effectiveness. It is essential to note that the ATPID damper was originally designed as an additional component to damp vibrations in the basic vibrating structure. Therefore, considering a larger grain mass is unjustified, as it would lead the damper to be treated as a fundamental dynamic structure, taking on a dominant role in the entire system dynamics. For smaller grain masses, the efficiency of the ATPID damper decreases non-linearly. Different damping efficiencies can be achieved for various vibration amplitudes. In the case of A_1 (represented by the black line), the maximum damping efficiency can be attained and reaches approximately 92% when the grain's mass equals 30% of the whole system's mass.

5. Conclusions

The Adaptive Tuned Particle Impact Damper is a damping device comprising granular material enclosed in a container of changeable high. Its crucial feature is the ability to dynamically adjust damping properties and effectively respond to real-time changes of operational condition. Methodology of designing an efficient ATPID damper involves several steps: experimental investigations, developing a mathematical model and employing optimization techniques. This paper extended previously analyzed issues to include the potential application of the Predictive Control Algorithm. Initially, this algorithm was conceived to narrow down the dataset range for faster optimal damper height search. Ultimately, it proved to be so efficient that it can determine optimal heights with a high effectiveness.

In this paper, we have commenced by delineating the overarching concept underlying the Predictive Control Algorithm (PCA). We have observed that the traditional method of theoretically determination of system dynamics necessitates proposing a numerical

model and possessing comprehensive knowledge about its parameters and applied excitations. The key principle of the PCA lies in overturning this classical paradigm. The initial phase of the algorithm entails prediction the vibrations of a given system in a specific state in the absence of complete system knowledge. Subsequently, utilizing the Predictive Control Algorithm facilitates the determination of the damper height when the initially identified type of vibrations is observed. Formulas enabling the estimation of the anticipated optimal height while adhering to the adopted assumptions describing the characteristics of optimal granulate motion were described in details. Following this, the article meticulously describes the implementation of the PCA algorithm in a real system, where knowledge of the system is confined to measured displacement of a cantilever beam's free end. The selected example showed that after 4 s of investigation, a damper's height close to the optimal one could be determined, and the beam vibration amplitude was reduced by 75% compared to the resonance vibration amplitude occurring for the case of deactivated damper.

Subsequent to this implementation, the algorithm's application in a system with available comprehensive information enabling its mathematical modeling and numerical simulation was presented. The sequential stages of the algorithm were elaborated upon, evidencing the possibility of rapid prediction of the damper height at which vibrations are effectively damped. Finally, an analysis of the PCA algorithm's sensitivity to variations in system parameters was presented. An experimental implementation of the PCA algorithm in a real mechanical system was proposed, where the excitation amplitude changed every 5 [s], taking on three different values. As a result of the PCA algorithm operation, it was possible to determine and set the optimal damper height for the current excitation within approximately 1.2 [s]. The algorithm enabled adaptive and effective tuning of the damper, thus ensuring efficient vibration reduction under varying operating conditions. Specifically, the influence of granulate mass, excitation amplitude, and gravity on the effectiveness of the PCA algorithm was studied. Greater grain mass and excitation amplitude lead to enhanced efficiency in accurately predicting the optimal damper's height. Moreover, it was observed that in various cases, the gravity phenomenon can be disregarded, thereby contributing to increased algorithmic efficiency.

The study presents a Predictive Control Algorithm designed to enhance the functionality of the Adaptive Tuned Particle Impact Damper by enabling rapid and efficient identification of the optimal damper height, even in systems with unknown dynamic characteristics. This approach overcomes the inefficiencies of traditional optimization methods, which typically require exhaustive and time-consuming numerical procedures. Real-time experimental implementation demonstrated that the algorithm is highly effective in reducing structural vibrations, while numerical simulations confirmed its performance in systems with known parameters. Sensitivity analysis revealed that grain mass and excitation amplitude are key factors affecting PCA accuracy. The proposed algorithm not only improves vibration mitigation efficiency but also significantly reduces the computational cost of finding the optimal height compared to traditional iterative simulations based solely on the governing equations. Future developments aim to incorporate artificial neural networks to further advance its predictive capabilities, positioning the PCA-enhanced ATPID as a cost-effective and versatile alternative to conventional dampers.

CRediT authorship contribution statement

Mateusz Żurawski: Writing – original draft, Validation, Methodology, Formal analysis, Conceptualization, Visualization, Project administration, Investigation, Data curation. **Cezary Graczykowski:** Writing – original draft, Validation, Investigation, Data curation, Writing – review & editing, Visualization, Supervision, Funding acquisition, Conceptualization. **Robert Zalewski:** Writing – review & editing, Supervision, Validation.

Declaration of competing interest

The authors declare the following financial interests/personal relationships which may be considered as potential competing interests: Cezary Graczykowski reports financial support was provided by National Science Centre Poland. If there are other authors, they declare that they have no known competing financial interests or personal relationships that could have appeared to influence the work reported in this paper.

Acknowledgments

Research was funded by the Warsaw University of Technology within the Excellence Initiative: Research University (IDUB) programme. The second author acknowledges the support of the National Science Centre, Poland, granted through the agreement 2018/31/D/ST8/03178.

Appendix

Symbols used in the paper are presented and described in Table 1.

Data availability

Data will be made available on request.

Table 1
The list of symbols.

Symbol	Description
x_s^d	System vibration in the damped state
x_{pred}^s	Predicted displacement of the ATPID lower wall (beam)
$\dot{x}_{pred}^s$	Predicted velocity of the ATPID lower wall (beam)
x_{pred}^h	Predicted displacement of the ATPID upper wall
$\dot{x}_{pred}^h$	Predicted velocity of the ATPID upper wall
$\ddot{x}_{pred}^s$	Acceleration of the ATPID lower wall (beam)
h_{max}	ATPID maximal damper height
A_{pred}	Predicted amplitude of the system vibration response
h_{pred}	Predicted ATPID damper height
t_{c_1}	Times of impact of the particle with the lower wall
t_{c_2}	Times of impact of the particle with the upper wall
t_c	Time of the contact
γ	The coefficient defining time of contact
T	One period of beam oscillation
X_g	The distance the grain moves between colliding the lower and upper walls in one vibration cycle
V_{k_0}	Initial velocity of the grain and
t_m	Measurement time
n	Number of the measured periods of the vibrations
x_s	System displacement
$\dot{x}_s$	System velocity
$\ddot{x}_s$	System acceleration
x_g	Grain displacement
$\dot{x}_g$	Grain velocity
$\ddot{x}_g$	Grain acceleration
u_s	Displacement of the harmonic excitation
$\dot{u}_s$	Velocity of the harmonic excitation
A	Excitation amplitude
f	Excitation frequency
M	Mass of the whole system
m_s	Reduced mass of the beam
k_s	Reduced stiffness of the beam
c_s	Reduced damping of the beam
m_g	Grain mass
g	Gravitational acceleration
r	Grain radius
x_{g_i}	Initial position of the grain
D_{red}	Reduced amplitude of a harmonic force excitation
f_0	Natural frequency of the system
A_0	First component of the Reduced amplitude of a harmonic force excitation
B_0	Second component of the Reduced amplitude of a harmonic force excitation
ω	Angular frequency of the excitation
ω_0	Natural angular frequency of the system
F_{c_1}	Contact force between grain and lower wall
F_{c_2}	Contact force between grain and upper wall
ξ_{c_1}	Overlap between grain and lower wall
ξ_{c_2}	Overlap between grain and upper wall
$\dot{\xi}_{c_1}$	Overlap rate of the grain collision with the lower wall
$\dot{\xi}_{c_2}$	Overlap rate of the grain collision with the upper wall
τ_{c_1}	Distance between the grain and the lower wall
τ_{c_2}	Distance between the grain and the upper wall
k_c	Reduced contact stiffness
c_c	Reduced contact damping
E_{eff}	Effective Young modulus
ν_w	Poisson's ratios of the wall
ν_g	Poisson's ratios of the grain
E_w	Young modulus of the wall
E_g	Young modulus of the grain
$\dot{h}$	Rate of the ATPID height changes
Δh	Control step
h_{old}	Container height computed in the last iteration
ψ	Control function
t_1	Activation start time
t_2	Saturation start time
t_{12}	Activation period
V_{grain}	Velocity of the grain (after the collision with the beam) in the PCA algorithm

(*continued on next page*)

Table 1 (*continued*).

V_{beam}	Velocity of the beam (after the collision with the grain) in the PCA algorithm
X_{grain}	Position of the grain (after the collision with the beam) in the PCA algorithm
X_{beam}	Position of the beam (after the collision with the grain) in the PCA algorithm
h_{opt}	Optimal damper height
Δh_{opt}	Effectiveness of the ATPID optimal height prediction by the PCA algorithm
d	Effectiveness of the ATPID damping
X_{ud}	Amplitude of undamped steady-state vibrations
X_{od}	Optimally damped steady-state vibrations

References

[1] Y. Hu, H. Zan, Y. Guo, J. Jiang, Z. Xia, H. Wen, Z. Peng, Energy dissipation characteristics of particle dampers with obstacle grids, Mech. Syst. Signal Process. 193 (2023) http://dx.doi.org/10.1016/j.ymssp.2023.110231.

[2] N. Meyer, R. Seifried, Energy dissipation in horizontally driven particle dampers of low acceleration intensities, Nonlinear Dynam. 108 (2022) http://dx.doi.org/10.1007/s11071-022-07348-z.

[3] C.C. Liao, Y. Chung, C. Weng, A study on the energy dissipation mechanism of dynamic mechanical systems with particle dampers by using the novel energy method, Nonlinear Dynam. 111 (2023) http://dx.doi.org/10.1007/s11071-023-08698-y.

[4] N. Meyer, R. Seifried, Damping prediction of particle dampers for structures under forced vibration using effective fields, Granul. Matter 23 (2021) http://dx.doi.org/10.1007/s10035-021-01128-z.

[5] N. Meyer, R. Seifried, Systematic design of particle dampers for transient vertical vibrations, Granul. Matter 25 (2022) http://dx.doi.org/10.1007/s10035-022-01290-y.

[6] J. Zhang, Y. Hu, J. Jiang, H. Zan, Damping characteristics of cantilever beam with obstacle grid particle dampers, Machines 10 (2022) http://dx.doi.org/10.3390/machines10110989.

[7] J. Dou, H. Yao, Y. Cao, S. Han, R. Bai, Enhancement of bistable nonlinear energy sink based on particle damper, J. Sound Vib. 547 (2023) http://dx.doi.org/10.1016/j.jsv.2022.117547.

[8] X. Li., A. Mojahed, C. Wang, L.Q. Chen, L.A. Bergman, A.F. Vakakis, Irreversible energy transfers in systems with particle impact dampers, Nonlinear Dynam. 110 (2024) http://dx.doi.org/10.1007/s11071-023-09007-3.

[9] A. Papalou, Effects of the design configuration on the performance of compartmental particle dampers, Int. J. Civ. Eng. 20 (2022) http://dx.doi.org/10.1007/s40999-022-00739-8.

[10] K. S., D. F., O. R., G. U., W. E., Partial filling of a honeycomb structure by granular materials for vibration and noise reduction, J. Sound Vib. 393 (2017) http://dx.doi.org/10.1016/j.jsv.2016.11.024.

[11] D. F., K. S., W. E., G. U., An effective vibration reduction concept for automotive applications based on granular-filled cavities, J. Vib. Control 24 (2018) http://dx.doi.org/10.1177/1077546316632932.

[12] P.B. B., D. F., J. D., W. E., Experimental study of particle dampers applied to wind turbine blades to reduce low-frequency sound emission, INTER- NOISE NOISE- CON Congr. Conf. Proc. 12 (2021) doi:/10.3397/IN-2021-1125.

[13] B.B. Prasad, F. Duvigneau, D. Juhre, E. Woschke, Damping performance of particle dampers with different granular materials and their mixtures, Appl. Acoust. 200 (2022) http://dx.doi.org/10.1016/j.apacoust.2022.109059.

[14] Q. Wang, D. Dan, A simplified modeling method for multi-particle damper: Validation and application in energy dissipation analysis, J. Sound Vib. 517 (2022) http://dx.doi.org/10.1016/j.jsv.2021.116528.

[15] F. Terzioglu, J.A. Rongong, C.E. Lord, Influence of particle sphericity on granular dampers operating in the bouncing bed motional phase, J. Sound Vib. 554 (2023) http://dx.doi.org/10.1016/j.jsv.2023.117690.

[16] X. Huang, W. Xu, W. Yan, J. Wang, Equivalent model and parameter analysis of non-packed particle damper, J. Sound Vib. 491 (2021) http://dx.doi.org/10.1016/j.jsv.2020.115775.

[17] X. Huang, W. Xu, J. Wang, W. Yan, Y. Chen, Equivalent model of a multi-particle damper considering particle rolling and its analytical solution, Struct Control. Heal. Monit. (2021) http://dx.doi.org/10.1002/stc.2718.

[18] X. Huan, X. Li, J. Wang, Optimal design of inerter-based nonpacked particle damper considering particle rolling, Earthq. Eng. Struct. Dyn. (2021) http://dx.doi.org/10.1002/eqe.3430.

[19] G. Wang, M. Faes, T. Shi, F. Cheng, Y. Pan, Investigation on impact behavior with viscous damping and tensile force inspired by kelvin-voigt model in granular system, Mech. Syst. Signal Process. (2025) http://dx.doi.org/10.1016/j.ymssp.2025.112399.

[20] B. Wang, H. He, S. Cheng, Y. Chen, Experimental and optimization analysis of a multiple unidirectional single-particle damper, J. Sound Vib. 553 (2023) http://dx.doi.org/10.1016/j.jsv.2023.117664.

[21] X. Huang, J. Miao, X. Li, Periodic motion and optimization design of non-stacked particle damper based on the double inert mass equivalent model, Earthq. Eng. Struct. Dyn. 53 (2024) doi:doi.org/10.1002/eqe.4050.

[22] M.A. Akbar, W.O. Wong, E. Rustighi, Design optimization of a single-mass impact damper, J. Sound Vib. 570 (2024) http://dx.doi.org/10.1016/j.jsv.2023.118019.

[23] D. Danhui, W. Qianqing, G. Jiongxin, Application of coupled multi-body dynamics—discrete element method for optimization of particle damper for cable vibration attenuation, Front. Struct. Civ. Eng. 15 (2021) http://dx.doi.org/10.1007/s11709-021-0696-x.

[24] Y. Wenzha, Z. Tiancong, Z. Shuini, N. Bo, T. Chenxuan, Y. Jiajie, H. Chao, M. Yong, Experimental studies on particle dampers with energy harvesting characteristics, J. Vib. Eng. Technol. (2023) http://dx.doi.org/10.1007/s42417-023-01000-9.

[25] Y. Harduf, E. Setter, M. Feldman, I. Bucher, Modeling additively-manufactured particle dampers as a 2DOF frictional system, Mech. Syst. Signal Process. 187 (2023) http://dx.doi.org/10.1016/j.ymssp.2022.109928.

[26] T. Ehlers, S. Tatzko, J. Wallaschek, R. Lachmayer, Design of particle dampers for additive manufacturing, Addit. Manuf. 38 (2021) http://dx.doi.org/10.1016/j.addma.2020.101752.

[27] T. Ehlers, R. Lachmayer, Design of particle dampers for laser powder bed fusion, Appl. Sci. 12 (2022) http://dx.doi.org/10.3390/app12042237.

[28] G. Honghu, K. Ichikawa, H. Sakai, H. Zhang, T. Akihiro, Numerical and experimental analysis in the energy dissipation of additively-manufactured particle dampers based on complex power method, Comput. Part. Mech. 10 (2023) http://dx.doi.org/10.1007/s40571-022-00540-3.

[29] X. Mengfei, X. Weibing, W. Jin, C. Yanjiang, Z. Daxing, H. Liqun, Y. Qiushi, Preliminary study on the damping effect of a rotational inertia particle damper considering the explosion response of continuous concrete bridges, Build. 13 (2023) http://dx.doi.org/10.3390/buildings13071726.

[30] L. Zheng, Z. Jiawei, W. Dianchao, Energy analysis of particle tuned mass damper systems with applications to MDOF structures under wind-induced excitation, J. Wind Eng. Ind. Aerodyn. 218 (2021) http://dx.doi.org/10.1016/j.jweia.2021.104766.

[31] B. shun Wang, H. xiang He, Y. fei Chen, S. tao Cheng, Experimental and performance analysis of the combined damping system with a TMD and a multiple unidirectional single-particle damper, J. Sound Vib. 540 (2022) http://dx.doi.org/10.1016/j.jsv.2022.117301.
[32] L. Wang, S. Nagarajaiah, Y. Zhou, W. Shi, Experimental study on adaptive-passive tuned mass damper with variable stiffness for vertical human-induced vibration control, Eng. Struct. (2023) http://dx.doi.org/10.1016/j.engstruct.2023.115714.
[33] L. Wang, W. Shi, Y. Zhou, Adaptive-passive tuned mass damper for structural aseismic protection including soil–structure interaction, Soil Dyn. Earthq. Eng. (2022) http://dx.doi.org/10.1016/j.soildyn.2022.107298.
[34] J. Salvi, F. Pioldi, E. Rizzi, Optimum tuned mass dampers under seismic soil-structure interaction, Soil Dyn. Earthq. Eng. 114 (2018) 576–597, http://dx.doi.org/10.1016/j.soildyn.2018.07.014.
[35] L. Wang, W. Shi, X. Li, Q. Zhang, Y. Zhou, An adaptive-passive retuning device for a pendulum tuned mass damper considering mass uncertainty and optimum frequency, Struct. Control. Heal. Monit. 26 (7) (2019) e2377, http://dx.doi.org/10.1002/stc.2377.
[36] L. Wang, W. Shi, Q. Zhang, Y. Zhou, Study on adaptive-passive multiple tuned mass damper with variable mass for a large-span floor structure, Eng. Struct. 209 (2020) 110010, http://dx.doi.org/10.1016/j.engstruct.2019.110010.
[37] K. Rong, Z. Lu, An improved ESM-fem method for seismic control of particle tuned mass damper in MDOF system, Appl. Acoust. (2021) 107663, http://dx.doi.org/10.1016/j.apacoust.2020.107663.
[38] L. Wang, S. Nagarajaiah, W. Shi, Y. Zhou, Study on adaptive-passive eddy current pendulum tuned mass damper for wind-induced vibration control, Struct. Des. Tall Spec. Build. (2020) http://dx.doi.org/10.1002/tal.1793.
[39] X. Ye, Y.-Q. Ni, M. Sajjadi, Y.-W. Wang, C.-S. Lin, Physics-guided, data-refined modeling of granular material-filled particle dampers by deep transfer learning, Mech. Syst. Signal Process. 180 (2022) http://dx.doi.org/10.1016/j.ymssp.2022.109437.
[40] Z. Yunan, G. Xiangying, W. Qian, C. Dongxing, A lightweight tuned particle damper for low-frequency vibration attenuation, J. Sound Vib. 583 (2024) http://dx.doi.org/10.1016/j.jsv.2024.118440.
[41] X. Ye, Y.-Q. Ni, W.K. Ao, L. Yuan, Modeling of the hysteretic behavior of nonlinear particle damping by Fourier neural network with transfer learning, Mech. Syst. Signal Process. 208 (2024) doi:doi.org/10.1016/j.ymssp.2023.111006.
[42] P. Veeramuthuvel, K. Sairajan, K. Shankar, Vibration suppression of printed circuit boards using an external particle damper, J. Sound Vib. 366 (2016) doi:doi.org/10.1016/j.jsv.2015.12.034.
[43] P. Veeramuthuvel, K. Shankar, K. Sairajan, Application of RBF neural network in prediction of particle damping parameters from experimental data, J. Vib. Control 23 (2017) http://dx.doi.org/10.1177/1077546315587147.
[44] P. Veeramuthuvel, K. Shankar, K. Sairajan, R. Machavaram, Prediction of particle damping parameters using RBF neural network, Procedia Mater. Sci. 5 (2014) doi:doi.org/10.1016/j.mspro.2014.07.275.
[45] S.F. Masri, Analytical and experimental studies of multiple-unit impact dampers, J. Acoust. Soc. Am. (1969) http://dx.doi.org/10.1121/1.1911581.
[46] S. Masri, Theory of the dynamic vibration neutralizer with motion-limiting stops, Earthq. Eng. Struct. Dyn. (1972) http://dx.doi.org/10.1115/1.3422718.
[47] S.F. Masri, R.K. Miller, T.J. Dehghanyar, T.K. Caughey, Active parameter control of nonlinear vibrating structures, J. Appl. Mech. (1989) http://dx.doi.org/10.1115/1.3176143.
[48] S.F. Masri, R. Ghanem, F. Arrate, J.P. Caffrey, A data-based procedure for analyzing the response of uncertain nonlinear systems, Struct. Control. Heal. Monit. (2009) http://dx.doi.org/10.1002/stc.322.
[49] Z. Lu, X. Lu, S. Masri, Studies of the performance of particle dampers under dynamic loads, J. Sound Vib. (2010) http://dx.doi.org/10.1016/j.jsv.2010.06.027.
[50] Z. Lu, S.F. Masri, X. Lu, Parametric studies of the performance of particle dampers under harmonic excitation, Struct. Control. Heal. Monit. (2011) http://dx.doi.org/10.1002/stc.359.
[51] Z. Lu, M. Zhou, J. Zhang, Z. Huang, S.F. Masri, A semi-active impact damper for multi-modal vibration control under earthquake excitations, Mech. Syst. Signal Process. 210 (2024) http://dx.doi.org/10.1016/j.ymssp.2024.111182.
[52] M. Żurawski, C. Graczykowski, R. Zalewski, The prototype, mathematical model, sensitivity analysis and preliminary control strategy for adaptive tuned particle impact damper, J. Sound Vib. 564 (2023) http://dx.doi.org/10.1016/j.jsv.2023.117799.
[53] M. Schwenzer, M., T. Bergs, D. Abel, Review on model predictive control: An engineering perspective, Int. J. Adv. Manuf. Technol. 117 (5) (2021) 1327–1349, http://dx.doi.org/10.1007/s00170-021-07682-3.
[54] J. Kohler, M.A. Muller, F. Allgower, Analysis and design of model predictive control frameworks for dynamic operation—An overview, Annu. Rev. Control. 57 (2024) 100929, http://dx.doi.org/10.1016/j.arcontrol.2023.100929.
[55] M.Q. Nguyen, M. Canale, O. Sename, L. Dugard, A model predictive control approach for semi-active suspension control problem of a full car, in: 2016 IEEE 55th Conf. on Decision and Control, CDC, Las Vegas, NV, USA, 2016, pp. 721–726, http://dx.doi.org/10.1109/CDC.2016.7798353.
[56] M.M. Morato, M.Q. Nguyen, O. Sename, L. D., Design of a fast real-time LPV model predictive control system for semi-active suspension control of a full vehicle, J. Franklin Inst. 356 (3) (2019) 1196–1224, http://dx.doi.org/10.1016/j.jfranklin.2018.11.016.
[57] X. Sun, C. Yuan, Y. Cai, S. Wang, L. Chen, Model predictive control of an air suspension system with damping multi-mode switching damper based on hybrid model, Mech. Syst. Signal Process. 94 (2017) 94–110, http://dx.doi.org/10.1016/j.ymssp.2017.02.033.
[58] A. Zahaf, S. Bououden, M. Chadli, M. Chemachema, Robust fault tolerant optimal predictive control of hybrid actuators with time-varying delay for industrial robot arm, Asian J. Control 24 (1) (2022) 1–15, http://dx.doi.org/10.1002/asjc.2444.
[59] K. Ishihara, J. Morimoto, An optimal control strategy for hybrid actuator systems: Application to an artificial muscle with electric motor assist, Neural Netw. 99 (2018) 92–100, http://dx.doi.org/10.1016/j.neunet.2017.12.010.
[60] D. Wu, H. Gu, H. Liu, GA-based model predictive control of semi-active landing gear, Chin. J. Aeronaut. 20 (1) (2007) 47–54, http://dx.doi.org/10.1016/S1000-9361(07)60006.
[61] C. Graczykowski, R. Faraj, Adaptive impact mitigation based on predictive control with equivalent mass identification, Sensors 23 (3) (2023) http://dx.doi.org/10.3390/s23239471.
[62] C. Graczykowski, R. Faraj, Extended identification-based predictive control for adaptive impact mitigation, Bull. Pol. Acad. Sci.: Tech. Sci. 71 (2023) http://dx.doi.org/10.24425/bpasts.2023.145937.
[63] M. Leblouba, Z.A. Al-Sadoon, S. Barakat, A. Fageeri, R. Awad, Assessing the performance of a novel granular material-based energy dissipation box damper for earthquake-resistant structures, J. Build. Eng. (2025) http://dx.doi.org/10.1016/j.jobe.2025.111999.
[64] F. Terzioglu, J.A. Rongong, Selection of granular damper parameters to achieve optimum vibration attenuation on vibrating structures, Mech. Syst. Signal Process. (2025) http://dx.doi.org/10.1016/j.ymssp.2025.112512.
[65] Z. Lu, Z. Wang, S.F. Masri, X. Lu, Particle impact dampers: Past, present, and future, Struct. Control. Heal. Monit. 25 (1) (2018) e2058, http://dx.doi.org/10.1002/stc.2058.
[66] L. Skrinjar, J. Slavic, M. Boltezar, A review of continuous contact-force models in multibody dynamics, Int. J. Mech. Sci. 145 (2018) 171–187, http://dx.doi.org/10.1016/j.ijmecsci.2018.07.010.
[67] H. Kruggel-Emden, E. Simsek, S. Rickelt, S. Wirtz, V. Scherer, Review and extension of normal force models for the discrete element method, Powder Technol. 171 (3) (2007) 157–173, http://dx.doi.org/10.1016/j.powtec.2006.10.004.